AUTHOR(S)
Al-waeel, M., Lukkari, J., Kivelä, H. & Salomäki, M.

TITLE
Heterogenous Copper(0)-Assisted Dopamine Oxidation: A New Pathway to Controllable and Scalable Polydopamine Synthesis

YEAR
2024

DOI
10.1021/acs.langmuir.4c02460

CITATION
Al-waeel, M., Lukkari, J., Kivelä, H. & Salomäki, M. (2024). Heterogenous Copper(0)-Assisted Dopamine Oxidation: A New Pathway to Controllable and Scalable Polydopamine Synthesis. *Langmuir*.
https://doi.org/10.1021/acs.langmuir.4c02460

VERSION
Accepted Manuscript

Heterogenous Copper(0)-Assisted Dopamine Oxidation: A New Pathway to Controllable and Scalable Polydopamine Synthesis

Majid Al-waeel, Jukka Lukkari, Henri Kivelä, Mikko Salomäki*

Department of Chemistry, University of Turku, FI-20014 Turku, Finland

mikko.salomaki@utu.fi

Abstract

In this study, we introduce an approach for synthesizing polydopamine (PDA) through the controlled oxidation of dopamine using metallic copper. Traditional methods of PDA synthesis often encounter challenges such as scalability, reproducibility, and control over polymerization. Our approach utilizes the catalytic properties of metallic copper in the presence of dissolved oxygen to generate reactive oxygen species (ROS) without additional chemicals. This process allows for precise control over dopamine oxidation, leading to reliable, materials and cost-effective upscalable PDA production. We investigated the reaction kinetics and the role of copper and ROS in dopamine oxidation, using several different experimental techniques. Our results demonstrate that, even at low pH, the copper-assisted method produces PDA with properties comparable to those synthesized through conventional means. We propose a mechanism for PDA synthesis that is initiated by oxygen adsorption onto copper surface, leading to the generation of various ROS which act as oxidizing agents in PDA synthesis. This method presents an advancement in the scalable and controlled production of PDA, with potential applications in various scientific and industrial fields.

Keywords: Polydopamine, Copper-assisted oxidation, Reactive oxygen species, Dopamine oxidation, Fenton-like reaction

Introduction

Since it was first reported, polydopamine (PDA), formed by the oxidation of the neurotransmitter dopamine, has opened promising innovative visions in the science of bioinspired materials.[1] In spite of its name it is not a real polymer but a complex mixture of different structural motifs connected by

covalent and noncovalent interactions.[2–4] The facile preparation and deposition, biocompatibility, and functional versatility of nanomaterials and coatings based on PDA and related materials have substantially advanced the application possibilities of biomimetic materials[5–8] including surface modification,[9] drug release,[10] heavy-metal capture,[11] and antioxidant activities[12]. Additionally, they offer irradiation protection,[13] and are studied for use in energy storage and harvesting[14–18]. In the field of biomedical research, PDA has applications in biosensors and bioanalysis,[19–21] bioimaging,[22] and photothermal therapy[23,24]. However, there are still some difficult fundamental unanswered questions that prevent the full realization of their potential, including a comprehensive understanding of the formation and adhesion mechanisms, the control of functionalization, and the reproducibility of synthesis and its effective upscaling beyond the laboratory scale.

The method of oxidation plays a pivotal role in chemical formation of PDA based materials[12,25,26], often dictating their functional properties. In most cases, the synthesis of PDA has been achieved via autoxidation, the use of atmospheric oxygen as an oxidant under alkaline conditions. The majority of the PDA autoxidation utilizes Tris(hydroxymethyl)aminomethane (Tris) buffer to obtain the alkaline pH of ca. 8.5, which method has established itself as the golden standard in polydopamine research. However, despite being an extremely simple method there are problems in the controllability and scalability. In addition, the Tris buffer may actively interfere in the PDA formation as the concentration of Tris has been found to play critical role in determining the resulting morphology[27] and electronic properties[28] of PDA. Moreover, the adhesive properties of polydopamine, a key factor for its wide range of applications, can also be influenced by the presence of Tris during synthesis, suggesting a nuanced role of Tris in affecting polydopamine's bonding capabilities.[29] Studies suggest that Tris, a primary amine, can become covalently incorporated into the polydopamine structure, thereby affecting the assembly and properties of the material.[29,30] In addition to atmospheric oxygen, other chemical oxidants, such as persulfate[31] and periodate[25], are often used. These oxidants have been shown to facilitate oxidation even under moderately acidic conditions. Although being fast, these oxidants may cause degradation of PDA.[25,32] Nevertheless, this degradation process can lead to enhanced hydrophilicity,[25] which can be advantageous in certain applications.

Redox-active transition metal ions can also be used as oxidants, with or without dissolved atmospheric oxygen.[33] Oxygen plays a role also in the UV irradiation induced oxidation[34] and in ozone-based oxidation[35]. In general, various reactive oxygen species (ROS) are very efficient oxidants formed in a large number of biological and chemical processes.[36] One important chemical route to ROS involves transition metal cations and Fenton-like reactions [37]. This reaction, which involves the catalytic decomposition of hydrogen peroxide usually by iron or copper ions to produce

hydroxyl radicals, represents an elegant yet powerful mechanism for generating highly reactive species. The Fenton reaction has potential to be self-sustaining, as the hydroxyl radicals it produces may regenerate hydrogen peroxide and the oxidation state of the metal ions. Studies have shown that that copper exhibits greater reactivity than iron in the Fenton-like reactions, and the reactions commence at submicromolar concentrations of hydrogen peroxide.[38,39] Iron-based Fenton reactions require acidic conditions, peaking in efficiency at a pH of 3.[40] Fenton-like reactions have also been applied to polydopamine synthesis. Especially, the Cu(II)/H_2O_2 pair has proven effective in oxidizing dopamine and facilitating the synthesis of PDA[41,42], the efficacy of the PDA formation being credited to the generation of ROS, likely hydroxyl radicals ($OH^{\bullet}$).[34,42] Additionally, UV irradiation promotes dopamine polymerization, effective even at a pH of 2, and the effect is further enhanced by the presence of H_2O_2 in the solution[34]. The introduction of ascorbic acid, a known ROS scavenger, inhibits polymerization, even under UV light, proving both Cu(II) and H_2O_2 alone as inefficient oxidants.[34] Copper(II) alone without added hydrogen peroxide can induce PDA formation, provided that chloride ions and oxygen are available, and the pH is above ca. 4.5.[43] The stabilization of the normally unstable copper(I) by chloride ions underpins their crucial role in the oxidative process.

The synthesis method affects the PDA structure and properties,[44,45] challenging standardization over various application fields, especially when aiming at large-scale production. In most applications, the material is needed as a thin coating on a substrate of choice. However, in traditional methods most PDA is formed in the solution and only a small fraction is deposited on a target substrate, leading to low material efficiency. Furthermore, the control of the dopamine oxidation process can be difficult due to its strong dependence on many experimental factors. The PDA films have complex molecular structure and the formation of a coating involves competing pathways of actual coating (film formation) and the self-aggregation in solution.[46] Therefore, it is difficult to determine the optimal timing and conditions for ensuring good adhesion and film quality, as adhesion is also found to be strongly related to oxidation state of the quinonoid products.[47] In electrodeposition, the pre-oxidation of dopamine to dopamine-*o*-quinone enhances the coating process.[48] This approach allows for the use of much lower precursor concentrations, at micromolar levels, thus increasing the reproducibility of the coating. On the other hand, film deposition by spraying[49,50] and electrospraying[51,52] have been proposed as alternatives for mass production due to their improved material efficiency, formation of uniform films, and the acceleration of the manufacturing process. However, these reported coating techniques employ stoichiometrically excessive amounts of oxidants or metal ions to accelerate the process, which combined with the rapid evaporation of solvents can introduce impurities in the films.

Electrospraying is a promising technique for upscaling the coating process, and we have searched for improved PDA formation methods to overcome the restrictions and problems discussed above. In this work, we present a well-controlled method for oxidizing dopamine to synthesize PDA. The primary goal has been to create stable, additive-free stock solutions of dopamine in a controlled oxidation and polymerization state, which would be ready for film deposition by spraying. This represents a cost-effective, material-efficient high-yield process suitable for industrial scale applications. Our method is extremely simple, employing only metallic copper (basically a common copper wire) in contact with stirred oxygen-containing water in an open vessel with dopamine hydrochloride as the only added component. The method relies on copper surface chemistry that generates ROS without the need of any additional chemicals. The exposure/withdrawal of copper metal to/from the solution provides an effective switch, which regulates the naturally occurring Fenton reactions in the solution.. Earlier research has established that copper is effective as a catalyst for the growth of polyaniline when used under ambient conditions.[53]

The process can be scaled and enhanced simply by adjusting the catalytic copper surface area and the oxygen content in the water. The method can potentially be expanded to an industrial-scale PDA production as it overcomes many limitations of the PDA synthesis and uses only very inexpensive materials under extremely simple experimental conditions. In this study, we evaluate the competence of this straightforward technique relative to various other documented methods for PDA production. We detail the process and explore its underlying mechanism, with connections to other PDA formation routes.

Materials and methods

Dopamine hydrochloride (Sigma-Aldrich), catechol (99%, Acros Organics), tris(hydroxymethyl)aminomethane (Tris, Sigma-Aldrich), sodium metaperiodate (Merck), copper (II) sulfate pentahydrate (Merck), 2,2,6,6-tetramethylpiperidine (TEMP; ≥99% purity, Sigma-Aldrich), 5,5-dimethyl-1-pyrroline N-oxide (DMPO; ≥98% purity, Sigma-Aldrich), coumarin (≥99% purity, Sigma-Aldrich), ethylenediaminetetraacetic acid disodium salt dihydrate (EDTA, VWR Chemicals), sodium acetate anhydrous (Merck), acetic acid (100%, Merck), hydrogen peroxide (30%, Sigma-Aldrich), hydrochloric acid (37%, VWR Chemicals), sulfuric acid (≥95%, Merck), perchloric acid (70%, VWR Chemicals), phosphoric acid (85%, Merck) were used as received. Double-distilled water was used for the preparation of aqueous solutions.

Copper metal pretreatment. Copper wires (Auremo, Finland) were cut and coiled to reach the surface areas of 5, 10, and 20 cm^2. The cut wires were immersed in concentrated sulfuric acid for 24 hours to remove any enamel coating. Following this, each wire was electrochemically polished at 3 V for 120 s in a 2-electrode cell, with the wire serving as the anode, a copper plate as the cathode and concentrated phosphoric acid as the electrolyte.[54] After electropolishing, the wires were thoroughly rinsed with deionized water to eliminate any remaining electrolyte residue. A different copper wire was used for each new experiment.

Copper-assisted synthesis of polydopamine. Dopamine hydrochloride was dissolved in 20 ml of deionized water to get a dopamine solution with a concentation of 5 mM. A copper wire was then suspended in the stirred solution for 72 hours. At defined intervals throughout the experimental timeline (0, 2, 4, 6, 24, 26, 30, 48, 50, 54, and 72 hours), aliquots were extracted from the solution for analysis. A volume of 75 µL was diluted to 0.125 mM for UV-Vis spectral analysis using a Cary 60 spectrophotometer (Agilent). Additionally, a 100 µL was diluted to a concentration range of 1-5 mg/L for atomic absorption spectroscopy analysis using Solaar M6 AA spectrometer (Thermo Scientific) equipped with a copper hallow cathode lamp and a deuterium background corrector. The flame was generated using an air–acetylene fuel. Identical experimental procedure was followed using either different dopamine concentrations 2.5, 10, and 20 mM or different solvents, such as acetate buffer solution (10 mM, pH 4.5) and perchloric acid (100 mM, pH 1). The pH value of each solution was measured using a multiparameter pH meter (Hanna Instruments).

Comparative study of polydopamine synthesis. Dopamine solutions, oxidized using four different oxidants $NaIO_4$(5 mM), $CuSO_4$, (5 and 25 mM) Tris(10 mM, pH 8.5), and copper metal, were allowed to react with their respective oxidant for 72 hours. Following the oxidation reaction, a 2 mL aliquot of each solution was diluted into 100 mL, and UV-Vis spectra were recorded. Additionally, another 2 mL aliquot of each solution was pipetted into a dialysis tube (3.5. kDa MWCO, 22 mm i.d., ThermoFisher), and dialyzed for 24 hours . The dialysis solution consisted of 250 mL of 1 mM HCl (pH 3), designed to remove any residuals of the oxidants especially copper ions. The dialysis solution was refreshed three times at the intervals of 2, 18, and 22 hours. Upon completion of the dialysis process, the contents of the dialysis tube were diluted into 100 mL, and UV-Vis spectra were recorded.

Electron Paramagnetic Resonance (EPR). Dopamine and catechol solutions were prepared at a concentration of 5 mM, whereas the DMPO and TEMP solutions were at concentrations of 50 mM and 10 mM respectively, with all solutes dissolved in deionized water. Immediately after the preparation of each solution, a 50 µL glass capillary tube was used to transfer an aliquot of the solution into the EPR instrument, a Magnettech miniscope MS-5000 spectrometer (Freiberg Instruments).

Data acquisition was performed with a modulation of 0.1 mT and a magnetic field frequency of 100 kHz. Microwave power was set to 10.00 mW, and the magnetic field was swept from 300.0 to 360.0 mT. The sweep time for the magnetic field was 60 seconds. Following the initial measurement, a copper wire was inserted into the capillary tube and the sample was measured again.

Photoluminescence. Dopamine and coumarin solutions were initially prepared at concentrations of 5 mM and 0.3 mM, respectively, the latter concentration being necessitated by coumarin's limited solubility in water. These stock solutions were subsequently diluted to a final concentration of 0.1 µM in a quartz cuvette. A copper wire was suspended in the cuvette, and was temporarily removed during the intervals when the beam passed through the cuvette, and reinserted afterward. Fluorescence emission measurements were conducted using a Photoluminescence Spectrometer FLS 1000 (Edinburgh Instruments), with the excitation wavelength set to 332 nm with a 1 nm bandwidth. The emission was detected at 455 nm.

X-ray photoelectron Spectroscopy (XPS). Dopamine solutions were drop-casted onto phosphorus-doped silicon wafers. XPS measurements were conducted using Thermo Scientific Nexsa XPS instrument, with a monochromatized Al Kα source, a pass energy of 50 eV, a spot size of 200 µm and dual mode charge compensation was on during all measurements. All XPS spectra were fitted with Thermo Scientific Avantage software, using the Avantage Smart background and a 30% mixed Gaussian/Lorentzian function. Carbon C1s C-C peak at 284.8 eV was set as the reference point for all peak fittings.

NMR spectroscopy. The ^{1}H NMR spectra were measured with a 500 MHz Bruker Avance III FT-NMR spectrometer (^{1}H: 500.12 MHz) equipped with a BB/^{1}H SmartProbe, with the sample temperature set at 2 °C. Approximately 5% D_2O (v/v) was added to the aqueous solutions for field-frequency lock and indirect (lock-signal-based) chemical shift referencing. The normal ^{1}H NMR spectra were measured with a single-pulse-acquire sequence using a 1 µs square RF pulse with ca. 3° flip angle, 0.3 s acquisition time, and 4.0 s relaxation delay, at 3.3 Hz FID resolution. Bruker's digitizer mode "baseopt" was used to ensure non-distorted baseline and optimal phase correction for quantitation. The selective ^{1}H NMR spectra were acquired with the Bruker pulse program selzg with 150k transients, using a 3.2 ms 90° Gaussian-shaped excitation pulse (truncated at 1%) centered at the H_2O_2 resonance frequency at ca. 11 ppm, with a 0.1 s acquisition time, 1 ms relaxation delay, and a spectral width of 6.0 ppm.

Results and discussion

Oxidation of dopamine with metallic copper. The effect of metallic copper on the oxidation of dopamine can be visually observed in a simple experiment. When an electropolished copper metal wire is immersed in an aqueous dopamine hydrochloride solution saturated with atmospheric oxygen, within hours a visible color change is observed as the solution becomes deep brownish (see fig. S1b). Dopamine (and all catechols) is a strongly complexing agent for copper(II) but if a nonoxidizable ligand, such as EDTA, is used a blueish color is seen (Fig. S1i). This color change is accompanied by the dissolution of copper into the solution as detected by Atomic Absorption Spectroscopy (AAS). Similar color changes are not seen with aqueous copper ion solution or without dissolved oxygen, indicating an oxygen-based surface reaction. During the process, the solution is vigorously stirred in an open vessel to ensure effective oxygen dissolution from ambient air and the distribution of the formed reactants. It should be noted that if heterogeneous reactions are involved the reaction kinetics is influenced by the surface area to solution volume ratio (A/V). Throughout our experiments, we maintained the solution volume constant at 20 cm^3, and the A/V ratio is directly proportional to the copper surface areas presented. The pH of an unbuffered 5 mM dopamine hydrochloride aqueous solution (pH = 5.15) is below the meaningful pH level required for the autoxidation of dopamine.[43]

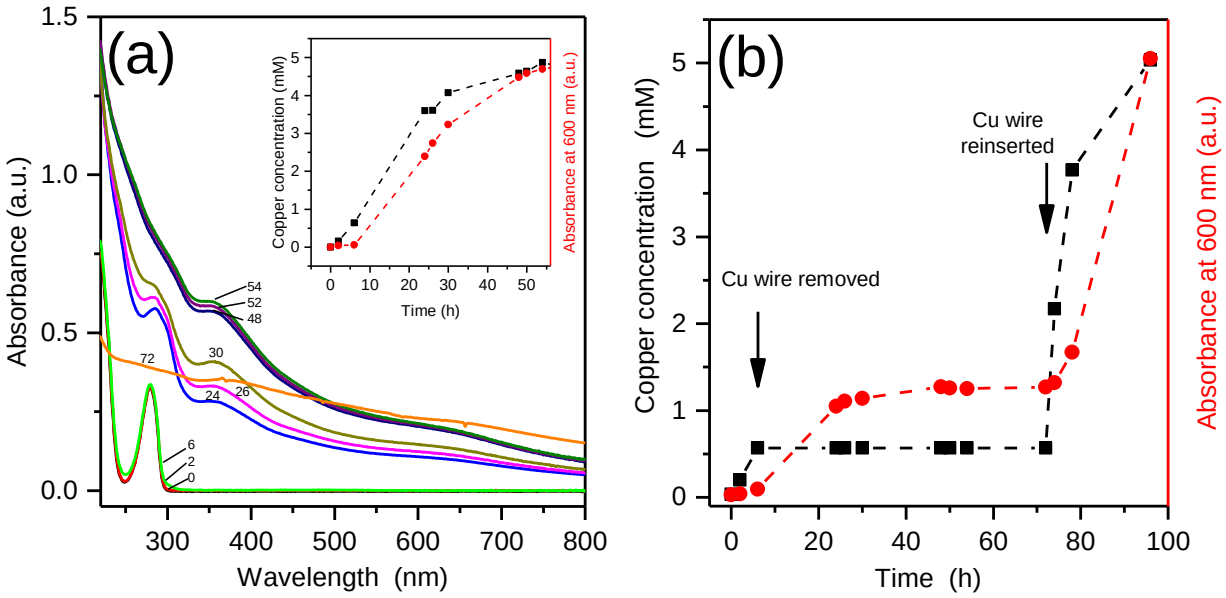

Figure 1. (a) Spectral changes upon inserting a copper wire into a 5 mM dopamine hydrochloride aqueous solution containing dissolved oxygen. Numbers indicate hours from the beginning of the reaction. Inset shows the absorbance at 600 nm and copper concentration over time. (b) The impact on absorbance and copper concentration when the copper wire is removed and reinserted. In both cases A/V = 0.25 cm^{-1}.

The dopamine oxidation to polydopamine and the dissolution of copper (total copper) were monitored using UV-visible spectroscopy and AAS, respectively. A typical sigmoidal pattern of absorbance and copper concentration growth over time is illustrated in the inset of Figure 1a, which also shows the whole spectral evolution during the process. We selected to follow the process at 600 nm, where the small-molecular intermediates in the PDA formation do not absorb but qualitatively similar curves are observed also at other wavelengths (see Fig. S2). The pivotal role of solid metallic copper in the reaction was highlighted in an experiment depicted in Figure 1b. Initially, with a copper wire in the solution, the dissolved copper concentration and absorbance start to rise. When the wire is removed the copper concentration, of course, remains constant. However, the absorbance at 600 nm continues to grow for about 20 hours before stabilizing at a constant value. This interval reflects the lifetime of the reactive oxygen species (ROS, see later) and intermediates formed before removal of the copper wire as they continue to produce PDA-type material. Upon reimmersing the copper wire, a rapid increase of both the copper concentration and absorbance is seen as the process restarts. Therefore, the copper wire acts as a kind of switch that enables to control the PDA formation in the solution. It should also be noted that material deposition on copper does not affect the PDA formation in solution (Fig. S3m).

The concentration of dissolved copper reaches a steady-state value close to that of the initial dopamine concentration in pure water, suggesting a near 1:1 stoichiometry in their interaction. However, the dissolution of copper is notably increased when the pH is reduced either through the addition of a strong acid or by using an acetate buffer (pH 4.5), (Fig. S3) which can be attributed to the effects of higher acidity or the specific action of buffer components; acetate, in particular, has been shown to facilitate copper dissolution.[55] In the presence of oxygen only, without dopamine or any other complexing agent, a minimal amount of copper dissolution was observed. On the other hand, if oxygen was removed from the solution only negligible copper dissolution or dopamine oxidation was observed (Fig. S3). These observations are in accordance with previous reports on copper dissolution in water.[56,57]

The spectral evolution during the process (Fig. 1a) is typical for the PDA generation. In order to verify that the product formed is similar polydopamine as prepared using traditional methods, the freshly synthesized drop-casted samples on silicon wafers were subjected to XPS spectroscopy analysis. The most informative XPS spectral region of PDA is the nitrogen N1s spectrum, which is usually characterized by three distinct peaks, each representing different amine functionalities. The first peak, around 402 eV, corresponds to primary amines ($R–NH_3^+$), typically found in PDA in variable quantities. The second peak, at approximately 400 eV, is linked to secondary amines (R–NH–R), or

indole groups, associated with both intermediate species and polydopamine and indicating the 5-ring closure. The third peak, around 398.5 eV, indicates tertiary or aromatic imino groups (=N–R), commonly seen in tautomeric species of 5,6-dihydroxyindole and 5,6-indolequinone.[58–60] The N1s spectrum of the PDA sample, prepared by using 5 mM dopamine hydrochloride with copper in double-distilled water, displayed all these characteristic amine moieties, and an additional peak at 401.2 eV (Fig. 2a). This peak is attributed to protonated imine (=NH^+-R). The protonation of the cyclic imine group is known to cause a +2.3 eV shift in the binding energy in analogous systems,[61] which matches the observed results. The wide peak near 405 eV in N1s spectrum is assigned to π -> π^* shake-up satellites.[62] The relative abundance of primary amines in the material is estimated to be approximately 10%, indicating that the synthesis has approached near to completion. Washing the drop-casted film with pH 3 HCl solution did not markedly change the N 1s spectrum of the material (Fig S4). The N1s XPS spectra of dopamine hydrochloride and 5,6-diacetoxyindole measured in powder form (Fig. S4) support the given assignations. Additionally, the obtained spectrum closely resembles the PDA spectra commonly reported in the literature.[58–60,63] This confirms that the copper-assisted method is an effective technique for generating material commonly referred to as polydopamine. The sample was also found to contain copper, with an approximate copper-to-nitrogen ratio of 1:1. The oxidation state of the copper in the film was analyzed using the Cu2p spectrum (Fig. 2b), which indicated the simultaneous presence of copper in both oxidation states, with the Cu(II):Cu(I) ratio of approximately 6:4. The copper content in the as-prepared polydopamine is similar to that observed when $CuSO_4$ was used as the oxidant in our earlier research.[64] PDA synthesis is usually restricted to alkaline or slightly acidic solutions because the Michael N-addition requires an unprotonated amine group. However, in Figure 2c we present the N1s spectrum for PDA synthesis at pH 1 (0.1 M $HClO_4$) using metallic copper. It shows characteristic peaks assigned to primary amines, secondary amines, and a minor peak suggesting the presence of imine moieties. The detection of secondary amines and imines implies the presence of closed ring structures, which make up slightly more than half of the nitrogen components after 48 hours of reaction. This finding challenges the conventional mechanistic understanding of PDA synthesis. Under typical conditions, the formation of leucodopaminechrome, with its characteristic secondary amine in closed five-membered ring structure, is considered unlikely at such a low pH due to the rate-limiting step of the Michael addition reaction [43,65]. This observation suggests that metallic copper may enable unique reaction pathways at low pH. In fact, other reported PDA syntheses at low pH suggest the role of radicals in cyclization reactions, although no detailed discussion of mechanisms is given.[34,66] While intriguing, a detailed exploration of the process at such a low pH is beyond the scope of the present study.

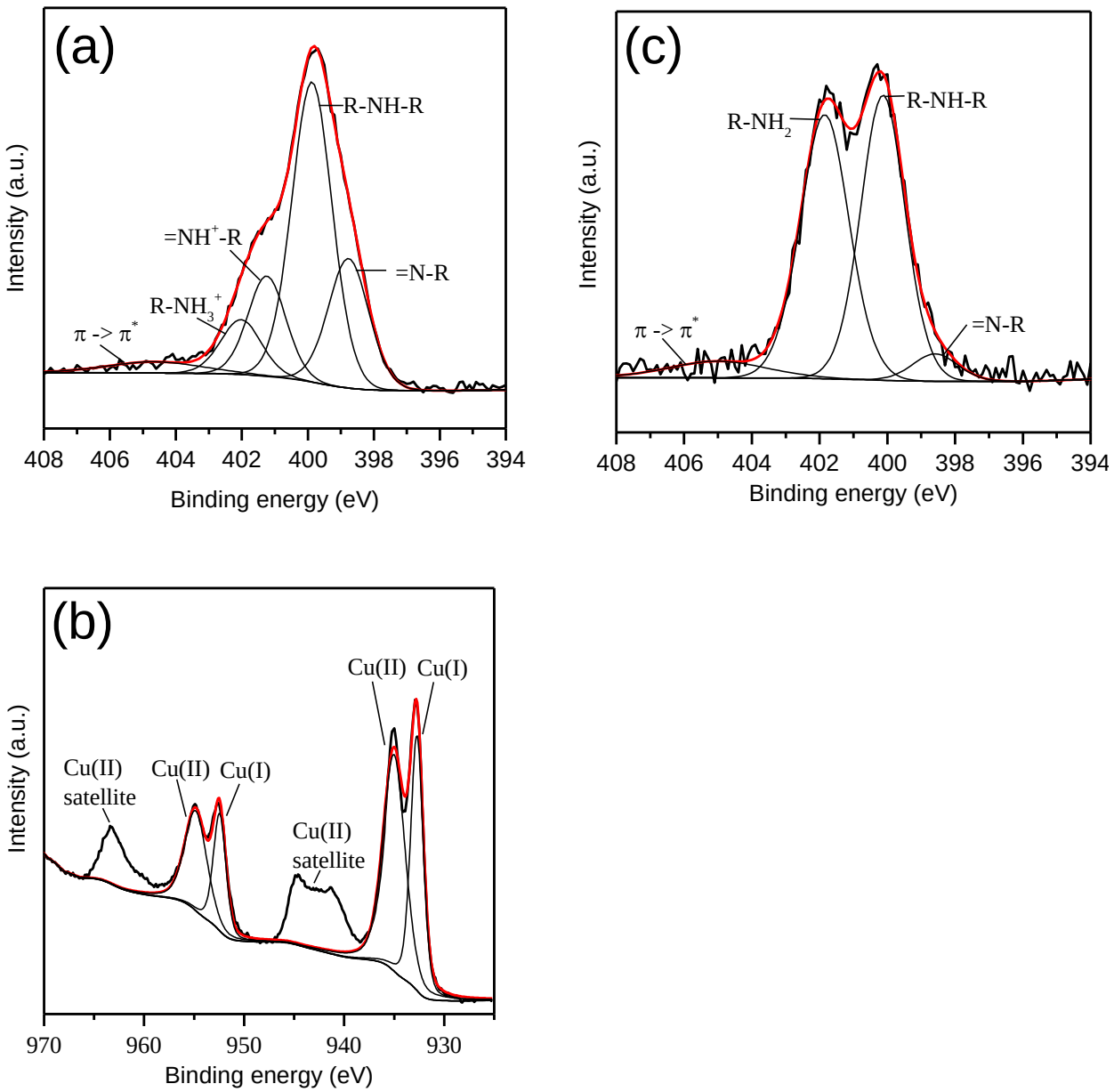

Figure 2. (a) N1s spectrum of a PDA sample prepared with metallic copper in oxygen-containing water, (b) Cu2p spectrum of the same sample, (c) N1s spectrum for PDA synthesis at pH 1. In all cases, dopamine hydrochloride concentration was 5 mM and A/V = 0.25 cm^{-1}.

Complementary to the XPS findings, UV-visible spectroscopy provided additional evidence of the intermediate species formed during the reaction. The spectra were deconvoluted to resolve overlapping absorption bands, which enables the identification of the species involved. The Supporting Information presents deconvoluted spectra and assignments of intermediates from various

oxidation methods, including copper-assisted oxidation in pure water and at pH 1, autoxidation in tris buffer, periodate oxidation, and Cu^{2+} + H_2O_2 oxidation (Fig. S5). All the studied systems displayed similar absorbance bands, suggesting the presence of the same intermediate species in different PDA generation methods (Tables S1 and S2). Specifically, bands attributed to aminochrome (AC) and 5,6-dihydroxyindole (DHI) were detected. The dopaminequinone (DQ) band at approximately 390 nm was absent in all copper-related methods, which can be attributed to a low concentration of this reactive intermediate. Additionally, all methods using copper displayed a band at ca. 350 nm, which is attributed to copper nanoparticles.[67] This band could be subsequently removed by dialysis, showing that copper is a removable component in the product. Any bands due to possible copper complexes were too weak to be reliably assigned.

The efficiency of the copper-assisted method compared to some well-established oxidation methods for polydopamine production is illustrated in Figure 3. In all cases the data refers to both the as-prepared product solutions and the samples dialyzed with a 3500 Da cut-off filter. This helps to see the differences in particle sizes and the relative amounts of unreacted dopamine monomers and small intermediates in the samples. While the $NaIO_4$ based oxidation is shown to be an effective method to produce large size products the as-produced samples by autoxidation in a Tris buffer and metallic copper in water have similar levels of material absorbing at 600 nm. However, dialysis shows that the metallic copper method produces smaller nanoparticles and/or molecular products. Copper ions in the as-produced sample were effectively removed by dialysis (inset of Fig. 3). Copper can also be removed by applying a water rinsing - centrifugation cycle three times. On the other hand, residual copper in the PDA sample may be beneficial in certain applications. For example, it has been shown that the incorporation of Cu(II) ions in PDA can result in antimicrobial properties, offering protection against pathogens.[68,69]

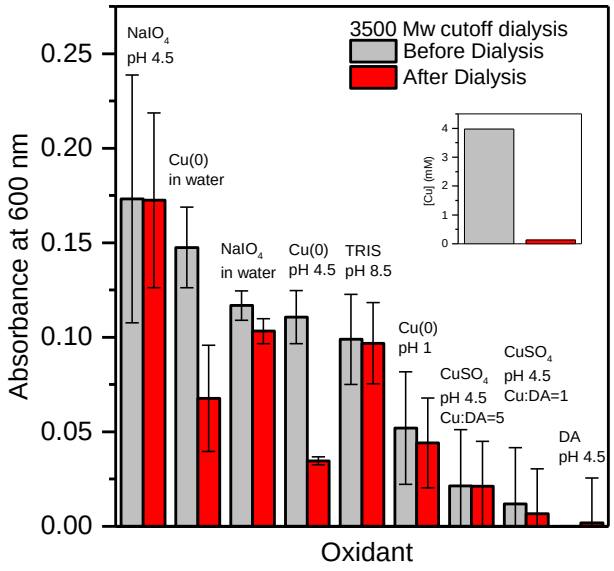

Figure 3. Comparison between copper-assisted and some traditional methods in polydopamine synthesis. The graph displays the absorbance at 600 nm after a 72-hour reaction period, with the inset indicating copper concentration changes in the sample using Cu(0) in double distilled water, before and after the dialysis. The error bars illustrate standard deviations from replicate measurements for the most prevalent PDA polymerization techniques ($NaIO_4$, tris, Cu(0) in water and Cu(0) at pH 4.5). For techniques with lower yield, a pooled standard deviation estimate from all polymerization experiments was applied.

***In-situ* detection of reactive oxygen species.** In the system comprising metallic copper, dopamine hydrochloride, water, and dissolved oxygen, there is no inherently active oxidant present. Atmospheric oxygen is an electronic triplet ($^3O_2$), a diradical with two unpaired electrons, which renders it relatively unreactive under standard conditions. The initiation step forming an active oxidant requires the activation of oxygen to generate more reactive species. Recent studies have documented the production of ROS by metallic copper in water, attributing the enhanced cytotoxicity to the more effective ROS generation on copper nanoparticles (NPs) compared to copper oxide NPs.[70] Covering the surface of copper NPs with long-chain thiols significantly reduces the ROS production, including hydrogen peroxide.[71] Notably, the generation of small amounts of hydrogen peroxide on copper surfaces in neutral aqueous solutions containing dissolved oxygen has been observed, leading to Cu(I) and Cu(II) species in water.[56] Copper is known for its capacity to produce ROS in aqueous environments through multiple mechanisms, including copper-oxygen surface complexes, copper dissolution following an intracomplex electron transfer, and subsequent Fenton-like reactions.[72] Notably, no hydrogen peroxide production or copper dissolution occurs when copper surfaces are

submerged in oxygen-free water[57]. A transient copper-oxygen surface species has been proposed to facilitate hydrogen peroxide formation on copper surfaces under acidic conditions[73].

In order to show that ROS are the probable candidates for oxidants in the metallic copper induced dopamine oxidation we have sought to detect their presence *in situ* in the reaction system. The most important ROS include hydroxyl radicals $OH^{\bullet}$, superoxide radicals ($O_2^{\bullet-}$ and $HOO^{\bullet}$), singlet oxygen $^1O_2$, and hydrogen peroxide H_2O_2. Hydroxyl radicals are extremely powerful oxidants, which react with most organic molecules at a diffusion controlled rate.[74,75] Coumarin can be used as a specific fluorometric probe for hydroxyl radicals.[76] Hydroxyl radicals react irreversibly with coumarin, yielding fluorescent 2-hydroxycoumarin, which serves as a cumulative indicator of radical formation. In an *in situ* experiment with metallic copper, dissolved oxygen, and dopamine hydrochloride in water, the 2-hydroxycoumarin fluorescence intensity at 455 nm initially rises slowly until its formation reaches a constant rate (Fig. 4a). Because of a large excess of coumarin in the solution this indicates that the hydroxyl radical concentration reaches a steady state in the solution. The high reactivity of hydroxyl radicals suggests them as primary oxidant in the system. Nonetheless, the significantly longer lifetime of superoxide radicals prevents the exclusion of their contribution, as the oxidation of dopamine (and semiquinone) by these radicals is thermodynamically feasible.[43]

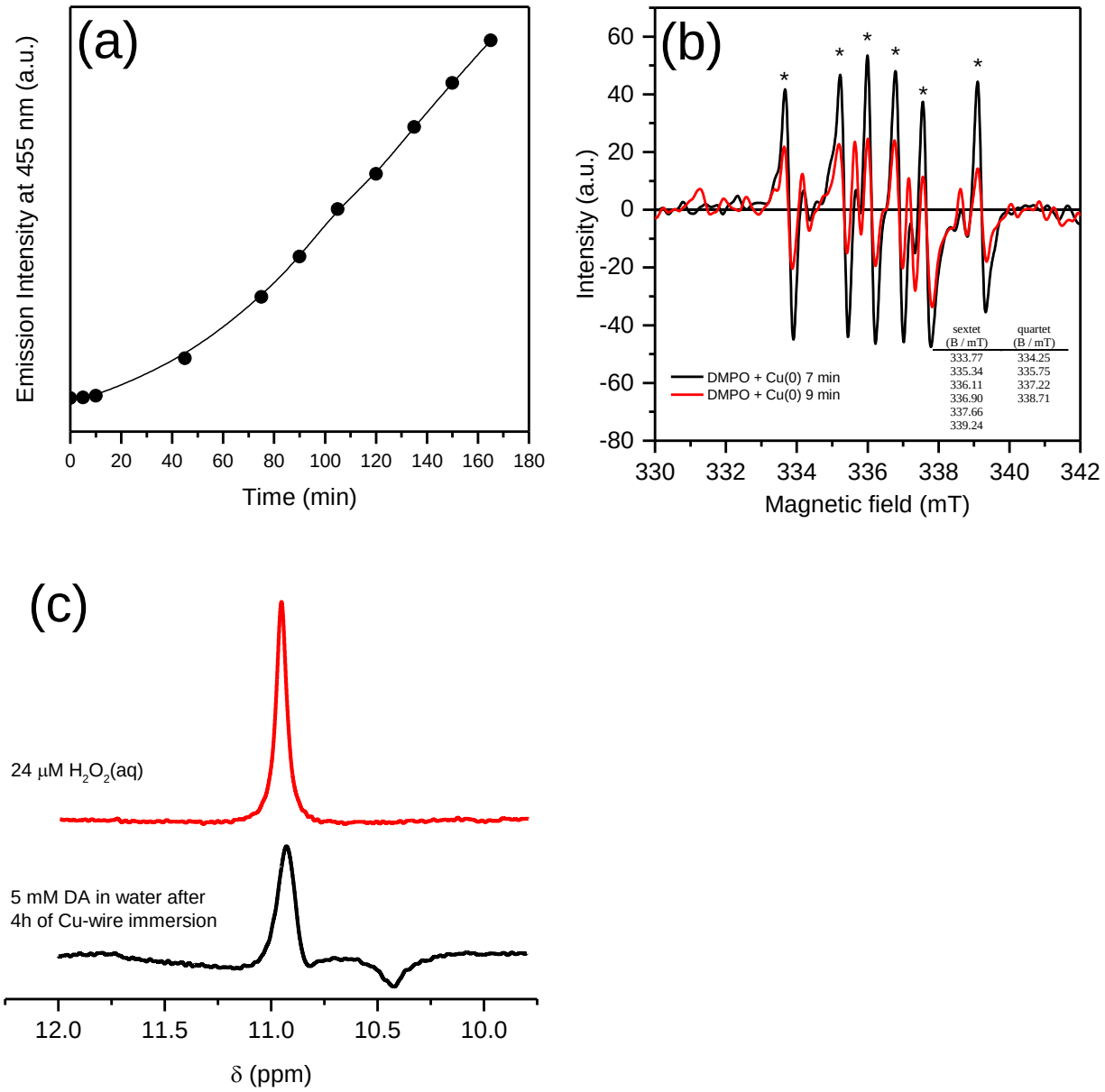

Figure 4: (a) Evolution of fluorescence at 455 nm indicating the formation of 2-hydroxycoumarin in a coumarin solution in the presence of dopamine, oxygen and metallic copper. (b) DMPO in water with metallic copper, with asterisks denoting signals attributed to the sextet. The inset shows the zero-crossing of the derivative signals corresponding to the peaks (at 9.5 GHz). (c) Selective ^{1}H NMR spectrum of dopamine solution after immersion of Cu wire (black) and a 24 μM H_2O_2(aq) reference solution (red) measured at 2 °C.

Another viable technique for ROS detection employs spin traps and EPR spectroscopy. DMPO (5,5-Dimethyl-1-pyrroline N-oxide) can be used as a radical scavenger as it forms adducts with short-lived free radicals and allows their stabilization and analysis. An *in situ* experiment with copper wire immersed in an aqueous solution containing DMPO shows the generation of radicals over time (Fig.

4b). Two different sets of peaks are observed, a sextet (marked with asterisks in Fig. 4b), which diminishes in intensity over time, and a quartet, which increases in intensity. The sextet is attributed to the coupling with ^{14}N (S = 1) and α-hydrogen (S = 1/2); it is more accurately described as a duodecet due to additional, weaker coupling with γ-hydrogen.[77–79] This multiplet has been assigned to the superoxide adduct of DMPO, probably due to two conformers. On the other hand, the reaction of the hydroxyl radical with DMPO is extremely fast, and results in a quartet in the ESR spectrum.[78,80] The progression observed in the DMPO EPR spectrum in Fig. 4b can be explained by the initial formation of superoxide adducts, which are subsequently replaced by hydroxyl radical adducts, suggesting a sequential formation of these ROS. In fact, the generation of hydroxyl radicals on copper-enriched surfaces in contact with oxygenated water has been reported.[78] If the solution contains dopamine or catechol (in addition to copper wire and DMPO) a weak multiplet with g-value characteristic for copper complexes starts to form at low field (Fig. S6a). This signal, which can be enhanced by the addition of H_2O_2, is not seen if the solution contains Cu(II) ions but not a copper wire. The multiplet grows in intensity with time and saturates after ca. 10 minutes, indicating that it corresponds to a transient species. Therefore, the most probable interpretation of the signal is a copper complex with some active oxygen species, formed close to the copper-solution interface.[81]

On the other hand, 2,2,6,6-tetramethylpiperidine (TEMP) is, typically, used for the spin trap detection of singlet oxygen in EPR. TEMP is a cyclic amine that reacts with singlet oxygen to form a detectable nitroxide radical, 2,2,6,6-tetramethylpiperidine-N-oxyl (TEMPO). However, a TEMPO signal can be observed, when TEMP is dissolved in a solvent, even if singlet oxygen is not present[82] . The signal intensity of TEMPO then decreases over time when copper metal and dopamine are introduced to the solution (Figure S6b). This signal decrease can be attributed to the oxidation of the TEMPO radical to TEMPOnium cation by the hydroperoxyl radical and superoxide radicals.[83] The TEMPO signal did not show any enhancement, suggesting that singlet oxygen could not be detected in the system.

Formation of hydrogen peroxide in the dopamine solution was directly detected with ^1H NMR spectroscopy, using a specific H_2O_2 quantification method.[84,85] In this method, the H_2O_2 ^1H resonance at ca. 11 ppm is selectively excited followed by rapid recovery of its z-magnetization via H_2O_2/H_2O hydrogen exchange, which allows quantitation of H_2O_2 down to sub-micromolar concentrations. The NMR spectrum of the 5 mM dopamine solution, after immersion of a copper wire (5 cm^2) for 4 hours, together with the spectrum of a 24 μM H_2O_2(aq) reference solution, are shown in Figure 4c. Hydrogen peroxide ^1H peak is clearly detected at ca. 10.9 ppm in the NMR spectrum of the dopamine solution, with an integral corresponding to a H_2O_2 concentration of ca. 17 μM, which implies an average net production of H_2O_2 under these conditions of ca. 60 nmol cm^{-2}. The 24 μM H_2O_2 reference solution

was diluted from a 0.12 M stock solution whose concentration was determined from the H_2O_2 and H_2O ^1H peak integrals by normal (non-selective) ^1H NMR spectroscopy. In water, H_2O_2 is a rather stable species but in the current system it is involved in various reactions, and therefore, the quantification is only approximate. This peroxide concentration is comparable to values reported on various water-solid surface interfaces.[86]

In summary, we have been able to detect three different emerging reactive oxygen species ($OH^{\bullet}$, superoxide, and peroxide), all effective oxidants, in the reaction system. Together with copper ions (both Cu(I) and Cu(II) ions), detected by AAS and XPS, they form the basis of an effective Fenton cycle chemistry in the system, and this allows us to further discuss the mechanism underlying the copper-induced dopamine oxidation and PDA formation.

Mechanism of dopamine oxidation and copper dissolution. There are several possible pathways for dopamine oxidation in the presence of ROS. In general, catechols undergo oxidation by diverse ROS under a variety of environmental conditions. For example, catechol polymerizes at the air/water interface through the action of hydroxyl radicals generated by ozone.[87] Among ROS, the hydroxyl radical stands out for its extreme reactivity, with a lifetime of approximately 1 ns and reacting with organic molecules at a diffusion-controlled rate.[88,89] Various ROS, notably superoxide radical and hydrogen peroxide, are produced via autoxidation of catechol, chemical oxidation, and metal-catalyzed oxidation processes.[40] The formation of singlet oxygen has been reported on molybdenum surfaces,[90] and with iron nanoparticles (FeNPs) and catechols confined in carbon nanotubes.[91] Singlet oxygen is a potent oxidant with a relatively long lifetime of 3.5 μs in distilled water,[92] but was not detectable in our system.

The interaction of hydroxyl radical with catecholamines may occur through hydrogen atom abstraction or radical addition mechanisms.[89] Hydrogen atom abstraction can proceed directly, by proton-coupled electron transfer (a simultaneous proton and electron transfer via a hydrogen bond), or by sequential electron-proton transfer. Theoretical and quantum mechanical transition-state calculations suggest that the abstraction from the catecholic hydroxyl groups is mediated by proton-coupled electron transfer at a diffusion-controlled rate, resulting in a semiquinone radical formation.[89] Additionally, rapid direct hydrogen abstraction is feasible at the α and β carbons of dopamine's alkyl side chain (excluding the protonated amino group). The protonated superoxide radical and the peroxyl radical engage with hydroxyl groups in dopamine through a similar mechanism but at a rate approximately four to five orders of magnitude slower, reflecting their significantly longer lifetime

in aqueous solutions.[89] First principle molecular dynamics calculations support the proton-coupled electron transfer pathway, indicating a competition with direct hydrogen abstraction in the case of the peroxyl radical.[93]

Based on literature and our observations we propose a mechanism, depicted in Scheme 1, involving the prompt adsorption of dissolved oxygen onto the copper surface. This initial step is followed by a corrosive electron transfer, resulting in the formation of copper(I) and superoxide. These species then engage in further redox reactions, including the creation of copper(II) and hydrogen peroxide. A key aspect of this mechanism is the adsorption of oxygen, which forms a surface complex.

(1) $\mathrm{Cu}^0 + n\mathrm{O}_2(\mathrm{aq}) \underset{k_{-ads}}{\overset{k_{ads}}{\rightleftharpoons}} \mathrm{Cu}\cdots n\mathrm{O}_2$

where $[\mathrm{O}_2] = \text{constant}$ and $n = \frac{1}{2}$ or 1; the smaller stoichiometric number for oxygen would be in accordance with the mechanism previously proposed,[94] and the observed order of the peroxide formation[95]. Formally, the two possibilities correspond to the different modes of bonding in the monocopper-oxygen complexes, either $\eta^1-\mathrm{O}_2$ (end-on, n = 1), or $\eta^2-\mathrm{O}_2$ (side-on, $n = \frac{1}{2}$).[96,97]

The interaction between copper and ROS may involve complex mechanisms comprising multiple elementary steps and intricate kinetics.[98,99] Nonetheless, for simplicity, we present the following steps as a simplified overview:

(2) $\mathrm{Cu}\cdots n\mathrm{O}_2 \underset{k_{-1}}{\overset{k_1}{\rightleftharpoons}} \mathrm{Cu}^+(\mathrm{aq}) + n\mathrm{SO}(\mathrm{aq})$

Because the pK_a value of superoxide $\mathrm{HOO}^{\cdot}$ is 4.8,[100] close to the actual pH of the reaction, we use a generic expression SO to notate both protonation forms; $\mathrm{SO} \triangleq \mathrm{O_2}^{\cdot -} + \mathrm{HOO}^{\cdot}$. In this heterogeneous process copper(I) ions and superoxide are formed in the solution close to the surface, within the diffusion layer. Their further redox reaction is energetically strongly favorable

(3) $\mathrm{Cu}^+(\mathrm{aq}) + \mathrm{SO}(\mathrm{aq}) \underset{k_{-2}}{\overset{k_2}{\rightleftharpoons}} \mathrm{Cu}^{2+}(\mathrm{aq}) + \mathrm{H_2O_2}$

The rate constant k_2 is very large, $\approx 10^9 - 10^{10}$ $\mathrm{M^{-1}\,s^{-1}}$, bringing it in the diffusion controlled regime.[101–105] On the other hand, the back reaction rate constant k_{-2} is significantly lower, of the order of $\approx 10^1 - 10^3$ $\mathrm{M^{-1}\,s^{-1}}$.[101,102,106–108] Because of the very fast forward reaction Cu(I) and SO may react already at the surface in an encounter complex geometry surrounded by the solvent shell, whereafter the products then diffuse to the vigorously stirred bulk of the solution. However, Cu(II) may also react with superoxide to give back Cu(I) and oxygen (the Haber-Weiss reaction)

(4) $\mathrm{Cu}^{2+}(\mathrm{aq}) + \mathrm{SO}(\mathrm{aq}) \xrightarrow{k_2'} \mathrm{Cu}^+(\mathrm{aq}) + \mathrm{O_2}(\mathrm{aq})$

The rate of this reaction decreases with the ionic strength and concentration of complexing agents (e.g., dopamine) in the solution but is practically diffusion controlled, close to that of reaction (3).[103–105]

The hydrogen peroxide formed can be decomposed by copper(I)[101,109–111]

$$(5)\quad Cu^{+}(aq) + H_2O_2 \xrightarrow{k_3} Cu^{2+}(aq) + OH^{\bullet} + OH^{-}$$

This is a rather slow reaction with the rate constant of the order of $k_3 \approx 10^2$ M^{-1} s^{-1}.[101] Some reports also suggest the generation of a very reactive copper(III) species in the reaction of copper(I) with hydrogen peroxide.[112] Further reactions may still produce hydroxyl radical, and experimental evidence points to hydroxyl radical being the major oxidizing agent produced in this reaction and the mechanism does not involve the highly reactive copper(III) species.[111] In heterogeneous catalysis, copper(I) species have the highest efficiency of hydroxyl radical generation from hydrogen peroxide.[113] The hydroxyl radical produced in this practically irreversible Fenton-like reaction is highly reactive, and in our case, we consider hydroxyl radical, detected by fluorescence and EPR, to be the major oxidizing agent. The superoxide radicals ($O_2^{\bullet -}$ and $HOO^{\cdot}$) can react rapidly with copper(I) after the initial electron transfer from copper to oxygen, and so the concentration of the radicals escaped into the bulk is low. In addition, they react at a considerably slower rate with dopamine than the hydroxyl radical, which is present in the bulk at a steady-state concentration.

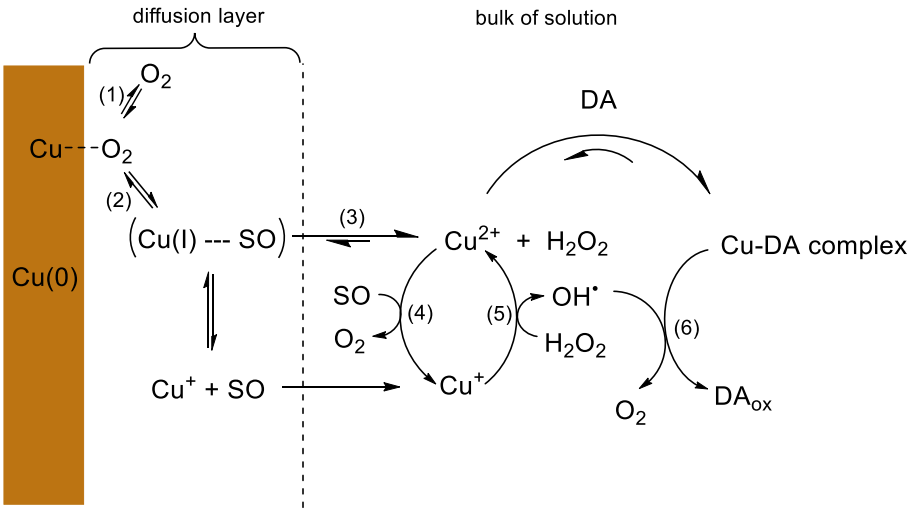

Scheme 1. Proposed mechanism for dopamine oxidation on copper surfaces

In the absence of dopamine (or other copper(II) complexing agents) the regeneration of copper(I) from copper(II) decelerates the overall dissolution rate of copper, once a steady state is reached. This phenomenon accounts for the minimal amount of dissolved copper under these conditions.[56] Conversely, in solutions containing strong complexing agents for copper(II), the formation of stable copper complexes serves as a sink for dissolved copper as long as free ligand is available. Copper complexes formed with oxygen and nitrogen ligands, despite their lability, exhibit significant stability. Such complexation holds back copper(II) from undergoing reactions that would otherwise lead to the generation of copper(I) and hinder dissolution rates. The role of metal complexation in enhancing metal dissolution and ROS production has been well-documented in previous studies.[114]

Metal dissolution is enhanced as long as any ligand capable of forming strong complexes with copper(II) is present in the solution. However, ligands that are redox-active undergo further reactions with the oxygen species produced, leading to a complex series of reactions. The dopamine oxidation mechanism described here is represented in Scheme 2. Dopamine and catechol are susceptible to oxidation by the hydroxyl radical through a mechanism involving hydrogen atom abstraction.

(6) $\mathrm{DA} + \mathrm{OH}^{\square} \xrightarrow{k_{OH}} \mathrm{DA}_{ox} + \mathrm{H_2O}$

In addition, as with all dopamine oxidation reactions involving oxygen the formed hydroxyl radical can also attack the catechol ring yielding radical adduct products.[89] When hydrogen abstraction occurs at the hydroxyl groups of dopamine, the resulting oxidized entity (DA_{ox}) is a dopamine semiquinone radical ($DSQ^{\bullet}$), which is not stable in aqueous solutions but disproportionates, yielding dopamine quinone (DQ) and regenerating dopamine.

(7) $2\mathrm{DSQ}^{\bullet} \rightarrow \mathrm{DQ} + \mathrm{DA}$

It may also react with dissolved oxygen to create dopamine quinone and more hydrogen peroxide[115]

(8) $\mathrm{DSQ}^{\bullet} + \mathrm{O_2} \rightarrow \mathrm{DQ} + \mathrm{SO} \xrightarrow{\mathrm{SO}} \mathrm{H_2O_2}$

The dopamine quinone formed can undergo the Michael N-addition, resulting in the creation of leucodopamine (DAL) characterized by a closed 5-ring structure.[43] Leucodopamine is further oxidized to dopaminechrome (DAC), which quickly tautomerizes into 5,6-dihydroxyindole (DHI). DHI can then be oxidized further to form indole quinone (IQ). On the other hand, hydrogen abstraction from the catechol ring may lead to the formation of either a dopamine semiquinone radical or its coupling with another radical, forming a dimer via C-C or C-O bonds. In every scenario, this series of reactions culminates in the production of what is commonly known as polydopamine.

(9) $\mathrm{DA}_{ox} \rightarrow \cdots \rightarrow \mathrm{PDA}$

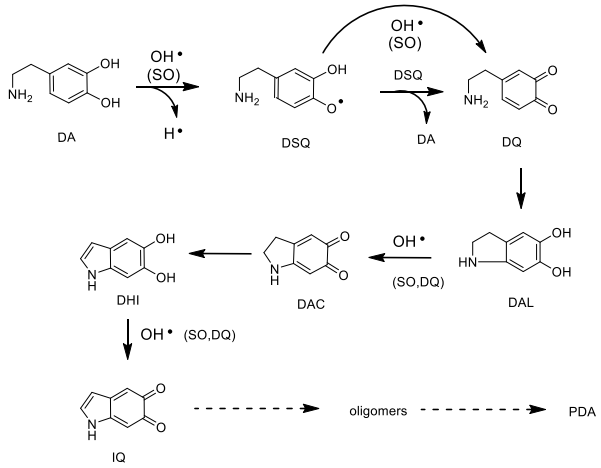

Scheme 2. Schematic polydopamine formation pathway (Cu complexes and OH-adduct formation not shown).

Kinetic analysis. The dopamine oxidation mechanism described above (Schemes 1 and 2) is an extremely complicated mechanism involving several feedback routes and is also basically an open reaction system. In addition, the presented individual steps may themselves hide complicated mechanisms. Many of the species are present in different protonation or complexation states, and possible rate constants would represent weighted averages of individual reactions. The presented scheme is also a simplified mechanism, where some possible reactions are omitted. Therefore, we follow a purely empirical approach to the kinetics of the polydopamine formation process. We chose to follow the process by absorbance at a wavelength where small intermediates do not absorb and attribute the absorbance to a chromophore assumed to be representative of polydopamine.

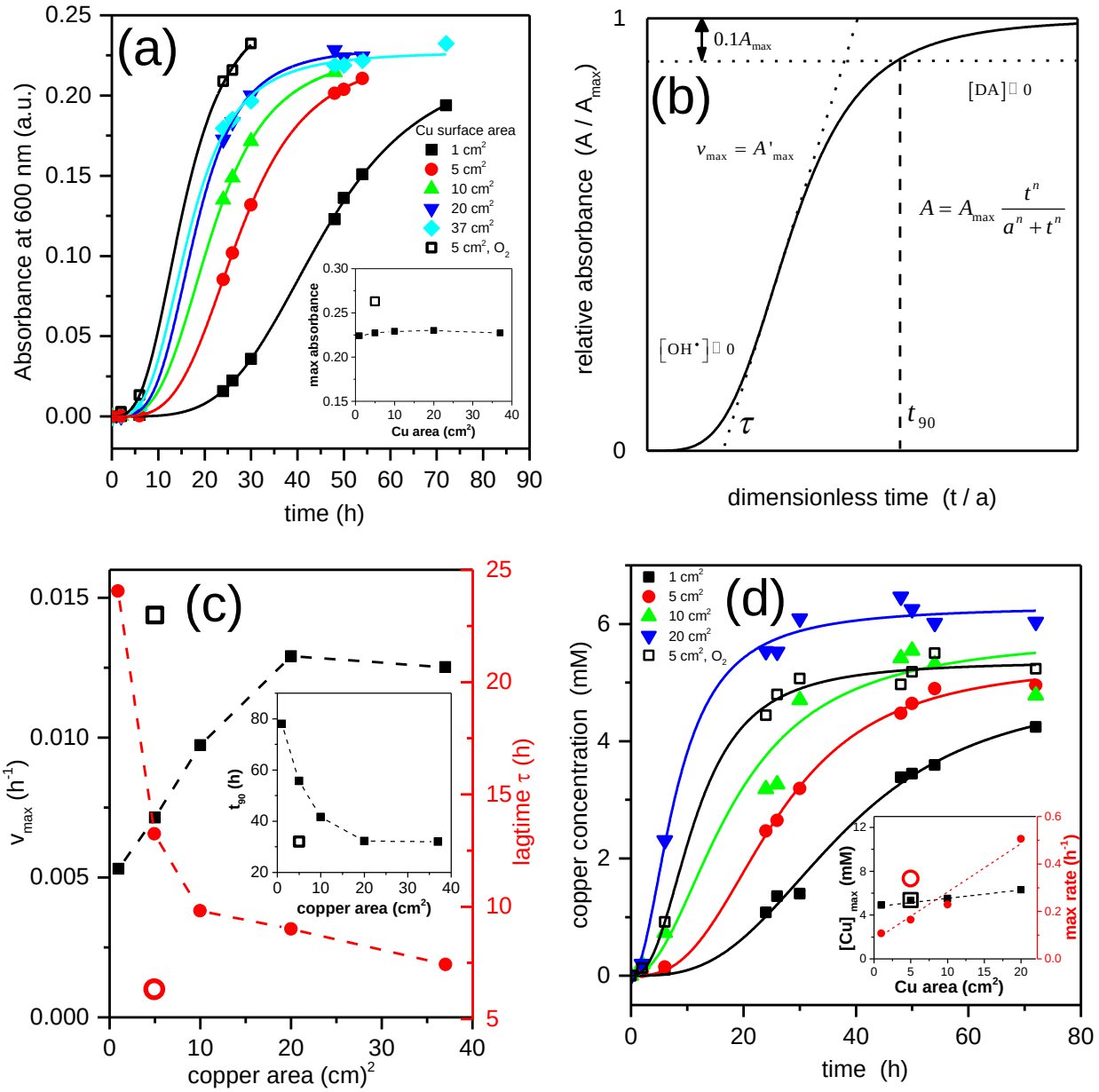

Figure 5. Evolution of absorbance (600 nm, solution diluted by a factor of 40) and copper concentration in water with immersed metallic copper and 5 mM dopamine:

(a) Absorbance at 600 nm as a function of time with different immersed copper surface areas. The inset shows the final absorbance. Open symbols represent the process in oxygen-saturated solutions.

(b) Parameters derived from the kinetic fit to the absorbance curves.

(c) Maximum rate and lag time as functions of copper surface area. The inset displays the time required for 90% completion. Open symbols represent a process in oxygen-saturated solutions.

(d) Time dependence of dissolved copper concentration with sigmoidal fits to the data. The inset shows the final copper concentration and the maximum rate of increase. Open symbols refer to a process under oxygen-saturated solutions.

The absorbance at 600 nm displays typical sigmoidal curves as a function of time (see Figs. 1a, 5a) for varying copper surface areas immersed in oxygen-containing pure water with 5 mM dopamine hydrochloride (pH 5). Initially, the reaction rate is low due to the minimal concentration of hydroxyl radicals (Fig. 5b). As the concentration of hydroxyl radicals reaches a steady state, it triggers the start of the reaction cascade, causing the reaction rate to accelerate. The process continues until all the dopamine is consumed, marking the completion of polydopamine formation. The final absorbance, depicted in the inset of Figure 5a, demonstrates its independence from the surface area of copper. It's noteworthy that further maturation of the material may occur subsequently at later times (see the last spectrum in Fig. 1a), and this process may not be well described by the sigmoidal time dependence. Moreover, the polydopamine aggregates and sedimentates at the bottom, as illustrated in case of the most rapidly ascending curves (Fig. S3), which restricts the time scale of the kinetic study. A general two-parameter (n, a) function that delineates a sigmoidal relationship of one variable (here absorbance, A) as a function of another (time, t) is[116]

$$A = A_{\max} \frac{t^n}{t^n + a^n} = \frac{A_{\max}}{1 + (a/t)^n}$$

This function (depicted in Fig. 5b) serves as simple method to represent and analyze sigmoidal behavior. We have identified four key parameters from the sigmoidal curve to characterize the process. The maximum absorbance ($A_{\max}$) indicates the quantity of material formed (within the followed time scale), and the maximum derivative of the curve represents the highest rate ($v_{\max}$) of the process. It's important to clarify that $v_{\max}$ pertains to the rate of product formation, rather than the early phase of the process involving copper dissolution and ROS generation. Additionally, the 90% completion time (t_{90}) is the time needed to achieve 90% of the maximum absorbance. The lag time (τ) is determined by the intersection of the time axis and the tangent line with the maximum slope, reflecting the initial period required to generate sufficient reactive species for effective polydopamine formation.

The maximum reaction rate shows a nearly linear correlation with the copper surface area immersed in water (Figure 5c) up to 20 cm². Beyond this point, increasing the surface area does not result in a further acceleration of the reaction. In addition, the lag time reaches a plateau with increasing copper surface area, which both imply that the rate of ROS production is no longer the rate-limiting step. The

maximum rate does not extrapolate to zero at a zero copper area because it pertains to the rate of product formation, not to the initial stages involving copper dissolution and ROS generation. Similarly, the time required to reach 90% completion (30 – 80 hours) stabilizes as the copper surface area exceeds approximately 10 cm^2 (corresponding to A/V ~ 0.5 cm^{-1}) (inset of figure 5c). Prior studies have demonstrated that hydrogen peroxide production on copper surfaces in water is proportional to the square root of oxygen concentration[56,72] . Under oxygen pressure of 1 atm (and at 25 °C) the solubility of oxygen in water is ca. 1.2 mM and approximately 0.26 mM from air (oxygen partial pressure 0.21 atm).[117] The experiments in solution saturated with pure oxygen (maintaining the solution under oxygen throughout the reaction) revealed that the ratio of the maximum rates for identical copper surface areas was almost equal to the square root of the solubility ratio, both for the absorbance increase and the copper dissolution (Figs. 5c, d). This finding corroborates the 1:0.5 stoichiometry of the surface mechanism (Cu + 1/2 O_2) and the η^2-O_2 nature of the surface oxygen complex. Both the initial lag time and the 90% completion time significantly decreased with increased oxygen concentration (Fig. 5c), although similar outcomes could be achieved by enlarging the copper surface area. Increase of the reaction rate (Fig. 5c) with pure oxygen also produces more absorbing material within the followed time scale without the need for further maturation of the mixture (see inset of Fig. 5a).

The copper dissolution displayed similar sigmoidal time dependence (Fig. 5d). Under ambient atmosphere, the dissolution rate depends linearly on the immersed copper surface area (inset of Fig. 5d). The use of pure oxygen atmosphere increases the copper dissolution rate but the not the amount of dissolved metal. Interestingly, the final copper concentration exhibits only a weak dependence on the surface area and tends to stabilize near the initial dopamine concentration (5mM), suggesting a complex formation between copper and catechol moieties with an approximate 1:1 stoichiometry. However, complexes between Cu(II) and catechol or dopamine have been identified at least in stoichiometries of 1:1 and 1:2,[118] and copper's potential to bind to nitrogen groups may further complicate the interaction[119]. Substituting catechol for dopamine in experiments revealed that final copper concentrations were about half of the initial catechol levels (Fig S3), implying the influence of the final product's structure. In polydopamine, typically only one complexing group per monomer, either catechol or primary amine, is available for binding due to the propensity to form supramolecular aggregates. Conversely, catechol oxidation products likely present less steric hindrance, accommodating metal complexes with variable stoichiometries. In any case, the results underscore the significance of complexation in driving copper dissolution.

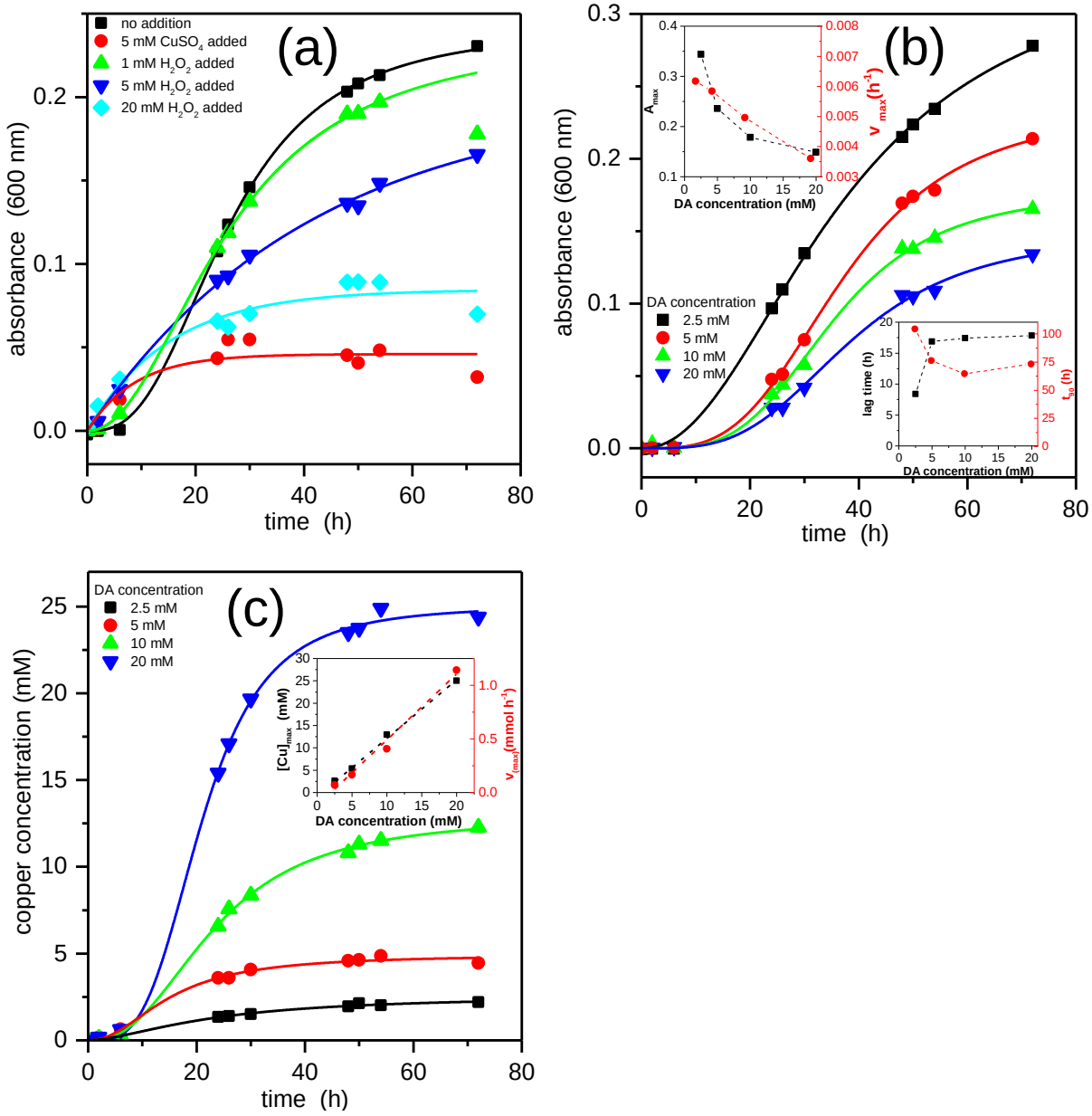

Figure 6. In (a), the rise of absorbance at 600 nm with different concentrations of added Cu(II) or H_2O_2. Immersed copper area 5 cm^2 and dopamine concentration 5 mM in each case. System with no added H_2O_2 and 1 mM H_2O_2 fitted with a sigmoidal function, others using an exponential function $A = A_{max}(1 - e^{-kt})$. Effect of dopamine concentration (in air, copper area 5 cm^2 in all cases) on (b) the absorbance (at 600 nm) and (c) the copper concentration. Insets show the effect on maximum absorbance and maximum rate, and lag time and 90% completion time. Absorbance refers to solutions diluted to a concentration of 0.125 mM

The combination of copper(II) ions and hydrogen peroxide has been found to be an efficient system for polydopamine synthesis[42]. This system's effectiveness is elucidated by the schematic mechanism depicted in Scheme 1, where the addition of these reagents shifts reaction (3) in reverse, generating

copper(I). Copper(I) then reacts with an excess of hydrogen peroxide to yield hydroxyl radicals, a process sustained as long as H_2O_2 is available, and typically the initial peroxide concentration is ca. four times than that of copper (usually 5 mM Cu(II) and 19.6 mM hydrogen peroxide). This observation led us to investigate the role of hydrogen peroxide (and copper ions) in the context of metallic copper in pure water, with outcomes presented in Figure 6a. The introduction of copper(II) or hydrogen peroxide alters the reaction dynamics significantly. The absorbance-time profiles deviate from the typical sigmoidal shape, except at the lowest peroxide concentration, by eliminating the initial lag phase, thereby allowing immediate commencement of the Fenton cycle and hydroxyl radical production without awaiting copper dissolution. Nonetheless, the process slows down with increasing hydrogen peroxide concentration. At the same time, the maximum product concentration diminishes, particularly at higher hydrogen peroxide levels or upon adding copper(II). The influence of additional copper and hydrogen peroxide can be justified by the suggested mechanism. Copper(II) itself acts as a relatively inefficient oxidant for dopamine, even when dissolved oxygen is present.[43] Furthermore, added copper(II) may reverse the ROS generating reactions and, crucially, bind all dopamine in the solution, preventing further dissolution of copper. This impedes the formation of copper(I) and the subsequent Fenton reactions that generate hydroxyl radicals.

On the other hand, the impact of added hydrogen peroxide is more complex. It reacts with dissolved copper(II) to produce copper(I) and increase hydroxyl radical production, shortening or, at higher hydrogen peroxide concentrations, entirely eliminating the initial lag phase of the process (see Fig. 6a). Nonetheless, the highly reactive hydroxyl radical can also attack and degrade the polydopamine and its precursors.[120] We propose that this degradation accounts for the reduced polydopamine yield at high peroxide concentrations, despite its rapid initial formation. Indeed, hydrogen peroxide has been shown to inhibit dopamine polymerization, with its effect on the polymerization rate levelling off at higher concentrations.[42] Thus, the rate of hydroxyl radical generation is pivotal for polydopamine synthesis, presenting a delicate balance between its beneficial role in dopamine oxidation and its detrimental effect on the polymer. In our studies, even the minimal (1 mM) added hydrogen peroxide concentration resulted in decreased yield.

The influence of oxygen on the process becomes evident when examining the impact of initial dopamine hydrochloride concentration (Figs. 6b and 6c; see also Fig. 5). The protonated amino group of dopamine hydrochloride, being a weak acid, does not markedly alter the pH within the studied concentration range. With a constant copper surface area, both the rate and quantity of copper dissolution linearly increase with dopamine concentration (inset of figure 6c). Notably, the final copper concentration is consistently about 30% higher than the initial dopamine concentration, suggesting a near 1:1 stoichiometry. However, the impact on polydopamine synthesis appears

paradoxical; both the final yield and formation rate of polydopamine decrease with increasing initial dopamine concentration (inset of figure 6b). This phenomenon is attributed to oxygen becoming a limiting factor at elevated dopamine concentrations. The primary oxidant, the hydroxyl radical, is generated through the interaction of dissolved oxygen with the copper surface. Thus, the oxidant-to-reactant ratio can be modulated either by altering the oxygen concentration in the solution (see Figure 5) or by adjusting the dopamine concentration. The highly reactive hydroxyl radical not only reacts with dopamine and other oxidizable species present but crucially with oxidized dopamine products as well. These latter reactions (Scheme 2) pave the way to polydopamine synthesis (unless the ROS concentration is too high, see above). Consequently, dopamine competes with its own oxidation products for hydroxyl radicals, and if oxidant production is the bottleneck, it initially hampers polydopamine formation. This limitation, however, is temporary and would diminish as dopamine is depleted if a continuous oxygen supply is guaranteed, but it affects the process on the time scale followed in Fig. 6b.

Conclusions

We have demonstrated a novel polydopamine formation method that uses only a well-agitated unbuffered oxygen-containing aqueous dopamine solution in contact with metallic copper, at room temperature and native pH, without any further added reagents. The copper-assisted method was found to be a viable, effective, and facile method for the synthesis of polydopamine (PDA). The intermediates in the reaction and the final product were identical to those in well-known polydopamine formation methods, including autoxidation. The oxidation of dopamine, facilitated by metallic copper, remained effective even at very low pH levels, suggesting that copper also catalyzes other, as yet unidentified, reaction pathways.

A detailed mechanism was proposed, wherein oxygen adsorbs onto the copper surface, initiating processes that result in the formation of copper(I) and superoxide. These species then undergo further redox reactions, producing copper(II) and hydrogen peroxide through Fenton-like reactions. Copper(I) is efficient in generating hydroxyl radicals from hydrogen peroxide, and the hydroxyl radical is considered to be the major oxidizing agent in this polydopamine synthesis, which does not require the addition of specific oxidants or any other reagents.

The quantitative formation of polydopamine exhibited sigmoidal time dependence, indicating that the reaction required the buildup of a sufficient ROS (mainly hydroxyl radical) concentration, after which the reaction rate accelerated until all dopamine was consumed. Increasing the immersed copper surface area to solution volume ratio enhanced the ROS generation, but only up to a certain limit, beyond which no further acceleration was observed, likely due to balancing of ROS generation on the surface and its consumption in the bulk of solution. Addition of copper ions or hydrogen peroxide had no direct benefit to the formation of PDA, besides the reduction of the initial lag time.

Future research will focus on assessing the scalability of this method for broader applications, specifically its potential for film deposition processes. The major benefits of the metallic copper based polydopamine synthesis are its extreme chemical and experimental simplicity, lack of excess oxidant salts in the product, and the possibility to generate stable stock solutions for electrospraying of polydopamine films. Work currently in progress has shown that the method produces well adherent films on a variety of substrates.

Acknowledgement

This work was supported by the M-ERA.net InsBIOration project, grant no. 100627561

Supporting Information

- Visual and spectroscopic assessments of dopamine oxidation.
- Detailed UV-Vis spectral fitting and analysis during polydopamine formation.
- N1s XPS spectra for reference compounds.
- ESR characterization of copper-dopamine interactions and singlet oxygen detection experiments.

References

(1) Lee, H.; Dellatore, S. M.; Miller, W. M.; Messersmith, P. B. Mussel-Inspired Surface Chemistry for Multifunctional Coatings. *Science (1979)* 2007, *318*, 426–430. https://doi.org/10.1126/science.1147241.

(2) Hong, S.; Na, Y. S.; Choi, S.; Song, I. T.; Kim, W. Y.; Lee, H. Non-Covalent Self-Assembly and Covalent Polymerization Co-Contribute to Polydopamine Formation. *Adv Funct Mater* 2012, *22* (22), 4711–4717.

(3) Liebscher, J.; Mrówczy´nski, R.; Scheidt, H. A.; Filip, C.; H\uadade, N. D.; Turcu, R.; Bende, A.; Beck, S. Structure of Polydopamine: A Never-Ending Story? *Langmuir* 2013, *29* (33), 10539–10548.

(4) Dreyer, D. R.; Miller, D. J.; Freeman, B. D.; Paul, D. R.; Bielawski, C. W. Elucidating the Structure of Poly(Dopamine). *Langmuir* 2012, *28* (15), 6428–6435.

(5) Ball, V. Polydopamine Nanomaterials: Recent Advances in Synthesis Methods and Applications. *Front Bioeng Biotechnol* 2018, *6* (AUG), 109. https://doi.org/10.3389/FBIOE.2018.00109/BIBTEX.

(6) Wang, S.; Cui, Y.; Dalani, T.; Sit, K. Y.; Zhuo, X.; Choi, C. K. Polydopamine-Based Plasmonic Nanocomposites: Rational Designs and Applications. *Chem. Commun.* 2024, *60* (22), 2982–2993. https://doi.org/10.1039/D3CC05883B.

(7) You, H.; Liu, X.; Li, Z.; Xie, M.; Wu, Y.; Wang, X.; Wang, Y.; Zeng, Q.; Wang, Z.; He, F. Recent Advances on the Construction of Multidimensional Polydopamine-Based Nanostructures. *Eur Polym J* 2023, *196*, 112319. https://doi.org/10.1016/J.EURPOLYMJ.2023.112319.

(8) Xu, Y.; Hu, J.; Hu, J.; Cheng, Y.; Chen, X.; Gu, Z.; Li, Y. Bioinspired Polydopamine Hydrogels: Strategies and Applications. *Prog Polym Sci* 2023, *146*, 101740. https://doi.org/10.1016/J.PROGPOLYMSCI.2023.101740.

(9) Lee, H. A.; Ma, Y.; Zhou, F.; Hong, S.; Lee, H. Material-Independent Surface Chemistry beyond Polydopamine Coating. *Acc Chem Res* 2019, *52* (3), 704–713. https://doi.org/10.1021/ACS.ACCOUNTS.8B00583/ASSET/IMAGES/MEDIUM/AR-2018-005835_0004.GIF.

(10) Menichetti, A.; Mordini, D.; Montalti, M. Polydopamine Nanosystems in Drug Delivery: Effect of Size, Morphology, and Surface Charge. *Nanomaterials* 2024, *14* (3), 303. https://doi.org/10.3390/nano14030303.

(11) Kim, D. J.; Ju, K.-Y.; Lee, J.-K. The Synthetic Melanin Nanoparticles Having an Excellent Binding Capacity of Heavy Metal Ions. *Bull Korean Chem Soc* 2012, *33* (11), 3788–3792.

(12) El Yakhlifi, S.; Alfieri, M.-L.; Arntz, Y.; Eredia, M.; Ciesielski, A.; Samorì, P.; d'Ischia, M.; Ball, V. Oxidant-Dependent Antioxidant Activity of Polydopamine Films: The Chemistry-Morphology Interplay. *Colloids Surf A Physicochem Eng Asp* 2021, 126134. https://doi.org/10.1016/j.colsurfa.2021.126134.

(13) Rageh, M. M.; El-Gebaly, R. H.; Abou-Shady, H.; Amin, D. G. Melanin Nanoparticles (MNPs) Provide Protection against Whole-Body E -Irradiation Pound in Mice via Restoration of Hematopoietic Tissues. *Mol Cell Biochem* 2015, *399* (1–2), 59–69.

(14) Khezraqa, H.; Safavi-Mirmahalleh, S. A.; Roghani-Mamaqani, H.; Salami-Kalajahi, M. A Review on Polydopamine as an Efficient Material in Different Components of Rechargeable Ion Batteries. *J Energy Storage* 2024, *79*, 110170. https://doi.org/10.1016/J.EST.2023.110170.

(15) Lee, G.; Kang, S.; Won, S. M.; Gutruf, P.; Jeong, Y. R.; Koo, J.; Lee, S.; Rogers, J. A.; Ha, J. S. Fully Biodegradable Microsupercapacitor for Power Storage in Transient Electronics. *Adv Energy Mater* 2017, *7* (18).

(16) Kim, Y. J.; Wu, W.; Chun, S.-E. S.-E.; Whitacre, J. F.; Bettinger, C. J. Biologically Derived Melanin Electrodes in Aqueous Sodium-Ion Energy Storage Devices. *Proceedings of the National Academy of Sciences* 2013, *110* (52), 20912–20917.

(17) Xu, R.; Gouda, A.; Caso, M. F.; Soavi, F.; Santato, C.; Casco, M. F.; Soavi, F.; Santato, C. Melanin: A Greener Route To Enhance Energy Storage under Solar Light. *ACS Omega* 2019, *4* (7), 12244–12251. https://doi.org/10.1021/acsomega.9b01039.

(18) Huang, Q.; Chen, J.; Liu, M.; Huang, H.; Zhang, X.; Wei, Y. Polydopamine-Based Functional Materials and Their Applications in Energy, Environmental, and Catalytic Fields: State-of-the-Art Review. *Chemical Engineering Journal* 2020, *387*, 124019. https://doi.org/10.1016/J.CEJ.2020.124019.

(19) Martín, M.; González Orive, A.; Lorenzo-Luis, P.; Hernández Creus, A.; González-Mora, J. L.; Salazar, P. Quinone-Rich Poly (Dopamine) Magnetic Nanoparticles for Biosensor Applications. *ChemPhysChem* 2014, *15* (17), 3742–3752.

(20) Li, D.; Luo, L.; Pang, Z.; Ding, L.; Wang, Q.; Ke, H.; Huang, F.; Wei, Q. Novel Phenolic Biosensor Based on a Magnetic Polydopamine-Laccase-Nickel Nanoparticle Loaded Carbon Nanofiber Composite. *ACS Appl Mater Interfaces* 2014, *6* (7), 5144–5151. https://doi.org/10.1021/am500375n.

(21) Ozlu, B.; Shim, B. S. Highly Conductive Melanin-like Polymer Composites for Nonenzymatic Glucose Biosensors with a Wide Detection Range. *ACS Appl Polym Mater* 2022, *4* (4), 2527–2535. https://doi.org/10.1021/acsapm.1c01818.

(22) Zhang, T.; Xu, H.; Wang, H.; Zhu, J.; Zhai, Y.; Bai, X.; Dong, B.; Song, H. Green Fluorescent Organic Nanoparticles Based on Carbon Dots and Self-Polymerized Dopamine for Cell Imaging. *RSC Adv* 2017, *7* (46), 28987–28993. https://doi.org/10.1039/c7ra03493h.

(23) Zmerli, I.; Michel, J. P.; Makky, A. Multifunctional Polydopamine-Based Nanoparticles: Synthesis, Physico-Chemical Properties and Applications for Bimodal Photothermal/Photodynamic Therapy of Cancer. *Multifunctional Materials* 2021, *4* (2), 022001. https://doi.org/10.1088/2399-7532/ABF0FA.

(24) Lin, L.-S.; Cong, Z.-X.; Cao, J.-B.; Ke, K.-M.; Peng, Q.-L.; Gao, J.; Yang, H.-H.; Liu, G.; Chen, X. Multifunctional Fe3O4@ Polydopamine Core–Shell Nanocomposites for Intracellular MRNA Detection and Imaging-Guided Photothermal Therapy. *ACS Nano* 2014, *8* (4), 3876–3883.

(25) Ponzio, F.; Barthès, J.; Bour, J.; Michel, M.; Bertani, P.; Hemmerlé, J.; d'Ischia, M.; Ball, V. Oxidant Control of Polydopamine Surface Chemistry in Acids: A Mechanism-Based Entry to Superhydrophilic-Superoleophobic Coatings. *Chemistry of Materials* 2016, *28* (13), 4697–4705.

(26) Ball, V.; Hirtzel, J.; Leks, G.; Frisch, B.; Talon, I. Experimental Methods to Get Polydopamine Films: A Comparative Review on the Synthesis Methods, the Films' Composition and Properties. *Macromol Rapid Commun* 2023, 2200946. https://doi.org/10.1002/MARC.202200946.

(27) García-Mayorga, J. C.; Rosu, H. C.; Jasso-Salcedo, A. B.; Escobar-Barrios, V. A. Kinetic Study of Polydopamine Sphere Synthesis Using TRIS: Relationship between Synthesis Conditions and Final Properties. *RSC Adv* 2023, *13* (8), 5081–5095. https://doi.org/10.1039/d2ra06669f.

(28) Della Vecchia, N. F.; Luchini, A.; Napolitano, A.; Derrico, G.; Vitiello, G.; Szekely, N.; Dischia, M.; Paduano, L. Tris Buffer Modulates Polydopamine Growth, Aggregation, and Paramagnetic Properties. *Langmuir* 2014, *30* (32), 9811–9818. https://doi.org/10.1021/la501560z.

(29) Tran, N. T.; Flanagan, D. P.; Orlicki, J. A.; Lenhart, J. L.; Proctor, K. L.; Knorr, D. B. Polydopamine and Polydopamine-Silane Hybrid Surface Treatments in Structural Adhesive Applications. *Langmuir* 2018, *34* (4), 1274–1286. https://doi.org/10.1021/acs.langmuir.7b03178.

(30) Della Vecchia, N. F.; Avolio, R.; Alfè, M.; Errico, M. E.; Napolitano, A.; d'Ischia, M. Building-Block Diversity in Polydopamine Underpins a Multifunctional Eumelanin-Type Platform Tunable Through a Quinone Control Point. *Adv Funct Mater* 2013, *23* (10), 1331–1340.

(31) Wei, Q.; Zhang, F.; Li, J.; Li, B.; Zhao, C. Oxidant-Induced Dopamine Polymerization for Multifunctional Coatings. *Polym Chem* 2010, *1* (9), 1430–1433.

(32) Yakhlifi, S. El; Ihiawakrim, D.; Ersen, O.; Ball, V. Enzymatically Active Polydopamine @ Alkaline Phosphatase Nanoparticles Produced by NaIO4 Oxidation of Dopamine. *Biomimetics* 2018, *3* (4). https://doi.org/10.3390/biomimetics3040036.

(33) Salomäki, M.; Ouvinen, T.; Marttila, L.; Kivelä, H.; Leiro, J.; Mäkilä, E.; Lukkari, J. Polydopamine Nanoparticles Prepared Using Redox-Active Transition Metals. *Journal of Physical Chemistry B* 2019, *123* (11). https://doi.org/10.1021/acs.jpcb.8b11994.

(34) Du, X.; Li, L.; Li, J.; Yang, C.; Frenkel, N.; Welle, A.; Heissler, S.; Nefedov, A.; Grunze, M.; Levkin, P. A. Uv-Triggered Dopamine Polymerization: Control of Polymerization, Surface Coating, and Photopatterning. *Advanced Materials* 2014, *26* (47), 8029–8033. https://doi.org/10.1002/adma.201403709.

(35) Tan, L.; Zhu, T.; Huang, Y.; Yuan, H.; Shi, L.; Zhu, Z.; Yao, P.; Zhu, C.; Xu, J. Ozone-Induced Rapid and Green Synthesis of Polydopamine Coatings with High Uniformity and Enhanced Stability. *Advanced Science* 2024, *11* (10). https://doi.org/10.1002/advs.202308153.

(36) Nosaka, Y.; Nosaka, A. Y. Generation and Detection of Reactive Oxygen Species in Photocatalysis. *Chemical Reviews*. American Chemical Society September 13, 2017, pp 11302–11336. https://doi.org/10.1021/acs.chemrev.7b00161.

(37) Goldstein, S.; Meyerstein, D.; Czapski, G. The Fenton Reagents. *Free Radic Biol Med* 1993, *15* (4), 435–445. https://doi.org/10.1016/0891-5849(93)90043-T.

(38) Millero, F. J.; Johnson, R. L.; Vega, C. A.; Sharma, V. K.; Sotolongo, S. Effect of Ionic Interactions on the Rates of Reduction of Cu(II) with H2O2 in Aqueous Solutions. *J Solution Chem* 1992, *21* (12), 1271–1287. https://doi.org/10.1007/BF00667222/METRICS.

(39) Kim, K.; Lee, K.; So, S.; Cho, S.; Lee, M.; You, K.; Moon, J.; Song, T. Fenton-Like Reaction between Copper Ions and Hydrogen Peroxide for High Removal Rate of Tungsten in Chemical Mechanical Planarization. *ECS Journal of Solid State Science and Technology* 2018, *7* (3), P91–P95. https://doi.org/10.1149/2.0131803JSS/XML.

(40) Zhang, Z.; He, X.; Zhou, C.; Reaume, M.; Wu, M.; Liu, B.; Lee, B. P. Iron Magnetic Nanoparticle-Induced ROS Generation from Catechol-Containing Microgel for Environmental and Biomedical Applications. *ACS Appl Mater Interfaces* 2020, *12* (19), 21210–21220. https://doi.org/10.1021/ACSAMI.9B19726/ASSET/IMAGES/LARGE/AM9B19726_0009.JPEG.

(41) Xu, Y.; Wang, W.; Zhu, Z.; Xu, B. In Situ Fenton Triggered Pda Coating Copper Mesh with Underwater Superoleophobic Property for Oily Wastewater Pretreatment. *Processes* 2021, *9* (9), 1665. https://doi.org/10.3390/PR9091665/S1.

(42) Zhang, C.; Ou, Y.; Lei, W. X.; Wan, L. S.; Ji, J.; Xu, Z. K. CuSO4/H2O2-Induced Rapid Deposition of Polydopamine Coatings with High Uniformity and Enhanced Stability. *Angewandte Chemie International Edition* 2016, *55* (9), 3054–3057. https://doi.org/10.1002/ANIE.201510724.

(43) Salomäki, M.; Marttila, L.; Kivelä, H.; Ouvinen, T.; Lukkari, J. Effects of PH and Oxidants on the First Steps of Polydopamine Formation: A Thermodynamic Approach. *J Phys Chem B* 2018, *122* (24), 6314–6327. https://doi.org/10.1021/acs.jpcb.8b02304.

(44) D'Ischia, M.; Napolitano, A.; Ball, V.; Chen, C. T.; Buehler, M. J. Polydopamine and Eumelanin: From Structure-Property Relationships to a Unified Tailoring Strategy. *Acc Chem Res* 2014, *47* (12), 3541–3550. https://doi.org/10.1021/ar500273y.

(45) Liebscher, J. Chemistry of Polydopamine - Scope, Variation, and Limitation. *European J Org Chem* 2019, *2019* (31–32), 4976–4994. https://doi.org/10.1002/ejoc.201900445.

(46) Lyu, Q.; Hsueh, N.; Chai, C. L. L. Direct Evidence for the Critical Role of 5,6-Dihydroxyindole in Polydopamine Deposition and Aggregation. *Langmuir* 2019, *35* (15), 5191–5201. https://doi.org/10.1021/acs.langmuir.9b00392.

(47) Alfieri, M. L.; Micillo, R.; Panzella, L.; Crescenzi, O.; Oscurato, S. L.; Maddalena, P.; Napolitano, A.; Ball, V.; D'Ischia, M. Structural Basis of Polydopamine Film Formation: Probing 5,6-Dihydroxyindole-Based Eumelanin Type Units and the Porphyrin Issue. *ACS Appl Mater Interfaces* 2018, *10* (9), 7670–7680. https://doi.org/10.1021/acsami.7b09662.

(48) Jaramillo, A. M.; Barrera-Gutiérrez, R.; Cortés, M. T. Synthesis, Follow-Up, and Characterization of Polydopamine-like Coatings Departing from Micromolar Dopamine- o-Quinone Precursor Concentrations. *ACS Omega* 2020, *5* (25), 15016–15027. https://doi.org/10.1021/acsomega.0c00676.

(49) Hong, S. H.; Hong, S.; Ryou, M.-H.; Choi, J. W.; Kang, S. M.; Lee, H. Sprayable Ultrafast Polydopamine Surface Modifications. *Adv Mater Interfaces* 2016, *3* (11), 1500857.

(50) Schlaich, C.; Li, M.; Cheng, C.; Donskyi, I. S.; Yu, L.; Song, G.; Osorio, E.; Wei, Q.; Haag, R. Mussel-Inspired Polymer-Based Universal Spray Coating for Surface Modification: Fast Fabrication of Antibacterial and Superhydrophobic Surface Coatings. *Adv Mater Interfaces* 2018, *5* (5). https://doi.org/10.1002/admi.201701254.

(51) Wang, J.; Pei, X.; Liu, G.; Han, Q.; Yang, S.; Liu, F. "Living" Electrospray – A Controllable Polydopamine Nano-Coating Strategy with Zero Liquid Discharge for Separation. *J Memb Sci* 2019, *586*, 170–176. https://doi.org/10.1016/j.memsci.2019.05.071.

(52) Geng, X.; Wang, J.; Ye, J.; Yang, S.; Han, Q.; Lin, H.; Liu, F. Electrosprayed Polydopamine Membrane: Surface Morphology, Chemical Stability and Separation Performance Study. *Sep Purif Technol* 2020, *244*, 116857. https://doi.org/10.1016/j.seppur.2020.116857.

(53) Gao, J.; Huang, J.; Huang, Z.; Meng, Q.; Zheng, L.; Sun, Q.; Li, G. Catalytic Growth of Highly Crystalline Polyaniline by Copper under Ambient Conditions. *CrystEngComm* 2018, *20* (35), 5119–5122. https://doi.org/10.1039/C8CE00893K.

(54) Van Gils, S.; Le Pen, C.; Hubin, A.; Terryn, H.; Stijns, E. Electropolishing of Copper in H3PO4. *J Electrochem Soc* 2007, *154* (3), C175. https://doi.org/10.1149/1.2429044.

(55) Singh, V. B.; Singh, R. N. Corrosion and Inhibition Studies of Copper in Aqueous Solutions of Formic Acid and Acetic Acid. *Corros Sci* 1995, *37* (9), 1399–1410. https://doi.org/10.1016/0010-938X(95)00042-I.

(56) Olszowka, S. A.; Manning, M. A.; Barkatt, A. Copper Dissolution and Hydrogen Peroxide Formation in Aqueous Media. *Corrosion* 1992, *48* (5), 411–418. https://doi.org/10.5006/1.3315954.

(57) Hedin, A.; Johansson, A. J.; Lilja, C.; Boman, M.; Berastegui, P.; Berger, R.; Ottosson, M. Corrosion of Copper in Pure O2-Free Water? *Corros Sci* 2018, *137*, 1–12. https://doi.org/10.1016/J.CORSCI.2018.02.008.

(58) Ding, Y.; Weng, L.-T.; Yang, M.; Yang, Z.; Lu, X.; Huang, N.; Leng, Y. Insights into the Aggregation/Deposition and Structure of a Polydopamine Film. *Langmuir* 2014, *30* (41), 12258–12269.

(59) Hemmatpour, H.; De Luca, O.; Crestani, D.; Stuart, M. C. A.; Lasorsa, A.; van der Wel, P. C. A.; Loos, K.; Giousis, T.; Haddadi-Asl, V.; Rudolf, P. New Insights in Polydopamine Formation via Surface Adsorption. *Nat Commun* 2023, *14* (1). https://doi.org/10.1038/s41467-023-36303-8.

(60) Zangmeister, R. A.; Morris, T. A.; Tarlov, M. J. Characterization of Polydopamine Thin Films Deposited at Short Times by Autoxidation of Dopamine. *Langmuir* 2013, *29* (27), 8619–8628.

(61) Stevens, J. S.; Byard, S. J.; Muryn, C. A.; Schroeder, S. L. M. Identification of Protonation State by XPS, Solid-State NMR, and DFT: Characterization of the Nature of a New Theophylline Complex by Experimental and Computational Methods. *Journal of Physical Chemistry B* 2010, *114* (44), 13961–13969. https://doi.org/10.1021/jp106465u.

(62) Kumar, S. N.; Gaillard, F.; Bouyssoux, G.; Sartre, A. High-Resolution XPS Studies of Electrochemically Synthesized Conducting Polyaniline Films. *Synth Met* 1990, *36* (1), 111–127. https://doi.org/10.1016/0379-6779(90)90240-L.

(63) Liu, T.; Kim, K. C.; Lee, B.; Chen, Z.; Noda, S.; Jang, S. S.; Lee, S. W. Self-Polymerized Dopamine as an Organic Cathode for Li- and Na-Ion Batteries. *Energy Environ Sci* 2017, *10* (1), 205–215. https://doi.org/10.1039/C6EE02641A.

(64) Salomäki, M.; Ouvinen, T.; Marttila, L.; Kivelä, H.; Leiro, J.; Mäkilä, E.; Lukkari, J. Polydopamine Nanoparticles Prepared Using Redox-Active Transition Metals. *Journal of Physical Chemistry B* 2019, *123* (11). https://doi.org/10.1021/acs.jpcb.8b11994.

(65) Umek, N.; Geršak, B.; Vintar, N.; Šoštarič, M.; Mavri, J. Dopamine Autoxidation Is Controlled by Acidic PH. *Front Mol Neurosci* 2018, *11*. https://doi.org/10.3389/fnmol.2018.00467.

(66) Zheng, W.; Fan, H.; Wang, L.; Jin, Z. Oxidative Self-Polymerization of Dopamine in an Acidic Environment. *Langmuir* 2015, *31* (42), 11671–11677.

(67) Dhineshbabu, N. R.; Rajendran, V.; Nithyavathy, N.; Vetumperumal, R. Study of Structural and Optical Properties of Cupric Oxide Nanoparticles. *Applied Nanoscience (Switzerland)* 2016, *6* (6), 933–939. https://doi.org/10.1007/s13204-015-0499-2.

(68) Yeroslavsky, G.; Richman, M.; Dawidowicz, L. O.; Rahimipour, S. Sonochemically Produced Polydopamine Nanocapsules with Selective Antimicrobial Activity. *Chemical Communications* 2013, *49* (51), 5721–5723. https://doi.org/10.1039/c3cc37762h.

(69) Hu, Z.; Wu, K.; Lin, J.; Tan, X.; Jiang, X.; Xiao, Y.; Xiang, L.; Yang, S.; Zhang, M.; Xu, W.; Chen, P. Synergistic Antibacterial Attributes of Copper-Doped Polydopamine Nanoparticles: An Insight into Photothermal Enhanced Antibacterial Efficacy. *Nanotechnology* 2024, *35* (15), 155102. https://doi.org/10.1088/1361-6528/ad19ad.

(70) Denluck, L.; Wu, F.; Crandon, L. E.; Harper, B. J.; Harper, S. L. Reactive Oxygen Species Generation Is Likely a Driver of Copper Based Nanomaterial Toxicity. *Environ Sci Nano* 2018, *5* (6), 1473–1481. https://doi.org/10.1039/C8EN00055G.

(71) Shi, M.; Kwon, H. S.; Peng, Z.; Elder, A.; Yang, H. Effects of Surface Chemistry on the Generation of Reactive Oxygen Species by Copper Nanoparticles. *ACS Nano* 2012, *6* (3), 2157–2164. https://doi.org/10.1021/NN300445D/SUPPL_FILE/NN300445D_SI_001.PDF.

(72) Kessler, A.; Hedberg, J.; Blomberg, E.; Odnevall, I. Reactive Oxygen Species Formed by Metal and Metal Oxide Nanoparticles in Physiological Media—A Review of Reactions of Importance to

Nanotoxicity and Proposal for Categorization. *Nanomaterials* 2022, *12* (11), 1922. https://doi.org/10.3390/NANO12111922.

(73) Colcleugh, D. W.; Graydon, W. F. The Kinetics of Hydrogen Peroxide Formation during the Dissolution of Polycrystalline Copper. *Journal of Physical Chemistry* 1962, *66* (7), 1370–1372. https://doi.org/10.1021/j100813a510.

(74) Charrier, J. G.; Anastasio, C. Rates of Hydroxyl Radical Production from Transition Metals and Quinones in a Surrogate Lung Fluid. *Environ Sci Technol* 2015, *49* (15), 9317–9325. https://doi.org/10.1021/ACS.EST.5B01606/SUPPL_FILE/ES5B01606_SI_001.PDF.

(75) Ervens, B.; Gligorovski, S.; Herrmann, H. Temperature-Dependent Rate Constants for Hydroxyl Radical Reactions with Organic Compounds in Aqueous Solutions. *Physical Chemistry Chemical Physics* 2003, *5* (9), 1811–1824. https://doi.org/10.1039/B300072A.

(76) Leandri, V.; Gardner, J. M.; Jonsson, M. Coumarin as a Quantitative Probe for Hydroxyl Radical Formation in Heterogeneous Photocatalysis. *Journal of Physical Chemistry C* 2019, *123* (11), 6667–6674. https://doi.org/10.1021/ACS.JPCC.9B00337/ASSET/IMAGES/LARGE/JP-2019-00337N_0008.JPEG.

(77) Clément, J. L.; Ferré, N.; Siri, D.; Karoui, H.; Rockenbauer, A.; Tordo, P. Assignment of the EPR Spectrum of 5,5-Dimethyl-1-Pyrroline N-Oxide (DMPO) Superoxide Spin Adduct. *Journal of Organic Chemistry* 2005, *70* (4), 1198–1203. https://doi.org/10.1021/JO048518Z/ASSET/IMAGES/LARGE/JO048518ZH00002.JPEG.

(78) Kim, J. K.; Metcalfe, I. S. Investigation of the Generation of Hydroxyl Radicals and Their Oxidative Role in the Presence of Heterogeneous Copper Catalysts. *Chemosphere* 2007, *69* (5), 689–696. https://doi.org/10.1016/J.CHEMOSPHERE.2007.05.041.

(79) Pieta, P.; Petr, A.; Kutner, W.; Dunsch, L. In Situ ESR Spectroscopic Evidence of the Spin-Trapped Superoxide Radical, O2−, Electrochemically Generated in DMSO at Room Temperature. *Electrochim Acta* 2008, *53* (8), 3412–3415. https://doi.org/10.1016/J.ELECTACTA.2007.12.018.

(80) Pei, S.; You, S.; Ma, J.; Chen, X.; Ren, N. Electron Spin Resonance Evidence for Electro-Generated Hydroxyl Radicals. *Environ Sci Technol* 2020, *54* (20), 13333–13343. https://doi.org/10.1021/ACS.EST.0C05287/ASSET/IMAGES/LARGE/ES0C05287_0006.JPEG.

(81) Kunishita, A.; Ishimaru, H.; Nakashima, S.; Ogura, T.; Itoh, S. Reactivity of Mononuclear Alkylperoxo Copper(II) Complex. O-O Bond Cleavage and C-H Bond Activation. *J Am Chem Soc* 2008, *130* (13), 4244–4245. https://doi.org/10.1021/JA800443S/SUPPL_FILE/JA800443S-FILE003.PDF.

(82) Nakamura, K.; Ishiyama, K.; Ikai, H.; Kanno, T.; Sasaki, K.; Niwano, Y.; Kohno, M. Reevaluation of Analytical Methods for Photogenerated Singlet Oxygen. *J. Clin. Biochem. Nutr* 2011, *49* (2), 87–95. https://doi.org/10.3164/jcbn.100125.

(83) Konopko, A.; Litwinienko, G. Mutual Activation of Two Radical Trapping Agents: Unusual “Win-Win Synergy” of Resveratrol and TEMPO during Scavenging of Dpph•Radical in Methanol. *Journal of Organic Chemistry* 2022, *87* (22), 15530–15538. https://doi.org/10.1021/acs.joc.2c02080.

(84) Kakeshpour, T.; Bax, A. NMR Characterization of H2O2 Hydrogen Exchange. *Journal of Magnetic Resonance* 2021, *333*. https://doi.org/10.1016/j.jmr.2021.107092.

(85) Kakeshpour, T.; Metaferia, B.; Zare, R. N.; Bax, A. Quantitative Detection of Hydrogen Peroxide in Rain, Air, Exhaled Breath, and Biological Fluids by NMR Spectroscopy. *Proc Natl Acad Sci U S A* 2022, *119* (8). https://doi.org/10.1073/pnas.2121542119.

(86) Eatoo, M. A.; Mishra, H. Busting the Myth of Spontaneous Formation of H2O2 at the Air-Water Interface: Contributions of the Liquid-Solid Interface and Dissolved Oxygen Exposed. *Chem Sci* 2024, *15* (9), 3093–3103. https://doi.org/10.1039/d3sc06534k.

(87) Guzman, M. I.; Pillar-Little, E. A.; Eugene, A. J. Interfacial Oxidative Oligomerization of Catechol. *ACS Omega* 2022, *7* (40), 36009–36016. https://doi.org/10.1021/ACSOMEGA.2C05290/ASSET/IMAGES/MEDIUM/AO2C05290_M003.GIF.

(88) Kehrer, J. P.; Robertson, J. D.; Smith, C. V. Free Radicals and Reactive Oxygen Species. *Comprehensive Toxicology: Second Edition* 2010, *1–14*, 277–307. https://doi.org/10.1016/B978-0-08-046884-6.00114-7.

(89) Iuga, C.; Alvarez-Idaboy, J. R.; Vivier-Bunge, A. ROS Initiated Oxidation of Dopamine under Oxidative Stress Conditions in Aqueous and Lipidic Environments. *Journal of Physical Chemistry B* 2011, *115* (42), 12234–12246. https://doi.org/10.1021/JP206347U/SUPPL_FILE/JP206347U_SI_001.PDF.

(90) Yi, Q.; Ji, J.; Shen, B.; Dong, C.; Liu, J.; Zhang, J.; Xing, M. Singlet Oxygen Triggered by Superoxide Radicals in a Molybdenum Cocatalytic Fenton Reaction with Enhanced REDOX Activity in the Environment. *Environ Sci Technol* 2019, *53* (16), 9725–9733. https://doi.org/10.1021/ACS.EST.9B01676/ASSET/IMAGES/LARGE/ES9B01676_0006.JPEG.

(91) Yang, Z.; Qian, J.; Yu, A.; Pan, B. Singlet Oxygen Mediated Iron-Based Fenton-like Catalysis under Nanoconfinement. *Proc Natl Acad Sci U S A* 2019, *116* (14), 6659–6664. https://doi.org/10.1073/PNAS.1819382116/SUPPL_FILE/PNAS.1819382116.SAPP.PDF.

(92) Ossola, R.; Jönsson, O. M.; Moor, K.; McNeill, K. Singlet Oxygen Quantum Yields in Environmental Waters. *Chem Rev* 2021, *121* (7), 4100–4146. https://doi.org/10.1021/acs.chemrev.0c00781.

(93) Milovanović, B.; Ilić, J.; Stanković, I. M.; Popara, M.; Petković, M.; Etinski, M. A Simulation of Free Radicals Induced Oxidation of Dopamine in Aqueous Solution. *Chem Phys* 2019, *524*, 26–30. https://doi.org/10.1016/J.CHEMPHYS.2019.05.001.

(94) Olszowka, S. A.; Manning, M. A.; Barkatt, A. Copper Dissolution and Hydrogen Peroxide Formation in Aqueous Media. *Corrosion* 1992, *48* (5), 411–418. https://doi.org/10.5006/1.3315954.

(95) Colcleugh, D. W.; Graydon, W. F. The Kinetics of Hydrogen Peroxide Formation during the Dissolution of Polycrystalline Copper. *Journal of Physical Chemistry* 1962, *66* (7), 1370–1372. https://doi.org/10.1021/j100813a510.

(96) Holland, P. L. Metal–Dioxygen and Metal–Dinitrogen Complexes: Where Are the Electrons? *Dalton Transactions* 2010, *39* (23), 5415.

(97) Elwell, C. E.; Gagnon, N. L.; Neisen, B. D.; Dhar, D.; Spaeth, A. D.; Yee, G. M.; Tolman, W. B. Copper-Oxygen Complexes Revisited: Structures, Spectroscopy, and Reactivity. *Chem Rev* 2017, *117* (3), 2059–2107. https://doi.org/10.1021/ACS.CHEMREV.6B00636/ASSET/IMAGES/MEDIUM/CR-2016-00636B_0044.GIF.

(98) Sawyer, D. T.; Valentine, J. S. How Super Is Superoxide? *Acc Chem Res* 1981, *14*, 393–400.

(99) Perez-Benito, J. F. Reaction Pathways in the Decomposition of Hydrogen Peroxide Catalyzed by Copper(II). *J Inorg Biochem* 2004, *98*, 430–438. https://doi.org/10.1016/j.jinorgbio.2003.10.025.

(100) Pham, A. N.; Xing, G.; Miller, C. J.; Waite, T. D. Fenton-like Copper Redox Chemistry Revisited: Hydrogen Peroxide and Superoxide Mediation of Copper-Catalyzed Oxidant Production. *J Catal* 2013, *301*, 54–64. https://doi.org/10.1016/J.JCAT.2013.01.025.

(101) Pham, A. N.; Xing, G.; Miller, C. J.; Waite, T. D. Fenton-like Copper Redox Chemistry Revisited: Hydrogen Peroxide and Superoxide Mediation of Copper-Catalyzed Oxidant Production. *J Catal* 2013, *301*, 54–64. https://doi.org/10.1016/J.JCAT.2013.01.025.

(102) Pham, A. N.; Waite, T. D. Cu(II)-Catalyzed Oxidation of Dopamine in Aqueous Solutions: Mechanism and Kinetics. *J Inorg Biochem* 2014, *137*, 74–84.

(103) Rabani, J.; Klug-Roth, D.; Lilie, J. Pulse Radiolytic Investigationes of the Catalyzed Disproportionation of Peroxy Radicals. Aqueous Cupric Ions. *Journal of Physical Chemistry* 1973, *77*, 1169–1175.

(104) Piechowski, M. Von; Nauser, T.; Hoignè, J.; Bühler, R. E. O−2 Decay Catalyzed by Cu2+ and Cu+ Ions in Aqueous Solutions: A Pulse Radiolysis Study for Atmospheric Chemistry. *Berichte der Bunsengesellschaft für physikalische Chemie* 1993, *97* (6), 762–771. https://doi.org/10.1002/BBPC.19930970604.

(105) Zafiriou, O. C.; Voelker, B. M.; Sedlak, D. L. Chemistry of the Superoxide Radical (O2-) in Seawater: Reactions with Inorganic Copper Complexes. *Journal of Physical Chemistry A* 1998, *102* (28), 5693–5700. https://doi.org/10.1021/JP980709G/SUPPL_FILE/JX5693.PDF.

(106) Perez-Benito, J. F. Reaction Pathways in the Decomposition of Hydrogen Peroxide Catalyzed by Copper(II). *J Inorg Biochem* 2004, *98*, 430–438. https://doi.org/10.1016/j.jinorgbio.2003.10.025.

(107) Millero, F. J.; Johnson, R. L.; Vega, C. A.; Sharma, V. K.; Sotolongo, S. Effect of Ionic Interactions on the Rates of Reduction of Cu(II) with H2O2 in Aqueous Solutions. *J Solution Chem* 1992, *21* (12), 1271–1287. https://doi.org/10.1007/BF00667222/METRICS.

(108) Millero, F. J.; Sharma, V. K.; Karn, B. The Rate of Reduction of Copper(II) with Hydrogen Peroxide in Seawater. *Mar Chem* 1991, *36*, 71–83.

(109) Gutteridge, J. M. C.; Wilkins, S. Copper Salt-Dependent Hydroxyl Radical Formation. Damage to Proteins Acting as Antioxidants. *BBA - General Subjects* 1983, *759* (1–2), 38–41. https://doi.org/10.1016/0304-4165(83)90186-1.

(110) Gunther, M. R.; Hanna, P. M.; Mason, R. P.; Cohen, M. S. Hydroxyl Radical Formation from Cuprous Ion and Hydrogen Peroxide: A Spin-Trapping Study. *Arch Biochem Biophys* 1995, *316*, 515–522.

(111) Eberhardt, M. K.; Ramirez, G.; Ayala, E. Does the Reaction of Cu + with H2O2Give OH Radicals? A Study of Aromatic Hydroxylation. *Journal of Organic Chemistry* 1989, *54* (25), 5922–5926. https://doi.org/10.1021/JO00286A024/ASSET/JO00286A024.FP.PNG_V03.

(112) Masarwa, M.; Cohen, H.; Meyerstein, D.; Hickman, D. L.; Bakac, A.; Espenson, J. H. Reactions of Low-Valent Transition-Metal Complexes with Hydrogen Peroxide. Are They “Fenton-like” or Not? 1. The Case of Cu+aq and Cr2+aq. *J Am Chem Soc* 1988, *110* (13), 4293–4297. https://doi.org/10.1021/JA00221A031/ASSET/JA00221A031.FP.PNG_V03.

(113) Sun, Y.; Tian, P.; Ding, D.; Yang, Z.; Wang, W.; Xin, H.; Xu, J.; Han, Y. F. Revealing the Active Species of Cu-Based Catalysts for Heterogeneous Fenton Reaction. *Appl Catal B* 2019, *258*, 117985. https://doi.org/10.1016/J.APCATB.2019.117985.

(114) Keenan, C. R.; Sedlak, D. L. Ligand-Enhanced Reactive Oxidant Generation by Nanoparticulate Zero-Valent Iron and Oxygen. *Environ Sci Technol* 2008, *42*, 6936–6941.

(115) Dellinger, B.; Pryor, W. A.; Cueto, R.; Squadrito, G. L.; Hegde, V.; Deutsch, W. A. Role of Free Radicals in the Toxicity of Airborne Fine Particulate Matter. *Chem Res Toxicol* 2001, *14* (10), 1371–1377. https://doi.org/10.1021/TX010050X/ASSET/IMAGES/LARGE/TX010050XF00005.JPEG.

(116) Dunning, A. J.; Kensler, J.; Coudeville, L.; Bailleux, F. Some Extensions in Continuous Models for Immunological Correlates of Protection. *BMC Med Res Methodol* 2015, *15*, 107. https://doi.org/10.1186/s12874-015-0096-9.

(117) Xing, W.; Yin, M.; Lv, Q.; Hu, Y.; Liu, C.; Zhang, J. Oxygen Solubility, Diffusion Coefficient, and Solution Viscosity. *Rotating Electrode Methods and Oxygen Reduction Electrocatalysts* 2014, 1–31. https://doi.org/10.1016/B978-0-444-63278-4.00001-X.

(118) Verastegui-Omaña, B.; Palomar-Pardavé, M.; Rojas-Hernández, A.; Corona Avendaño, S.; Romero-Romo, M.; Ramírez-Silva, M. T. Spectrophotometric Quantification of the Thermodynamic Constants of the Complexes Formed by Dopamine and Cu(II) in Aqueous Media. *Spectrochim Acta A Mol Biomol Spectrosc* 2015, *143*, 187–191. https://doi.org/10.1016/J.SAA.2015.01.067.

(119) Hong, L.; Simon, J. D. Current Understanding of the Binding Sites, Capacity, Affinity, and Biological Significance of Metals in Melanin. *J Phys Chem B* 2007, *111* (28), 7938–7947.

(120) Lin, J.-H.; Yu, C.-J.; Yang, Y.-C.; Tseng, W.-L. Formation of Fluorescent Polydopamine Dots from Hydroxyl Radical-Induced Degradation of Polydopamine Nanoparticles BT - Physical Chemistry Chemical Physics. June 2, 2015, pp 15124–15130. http://pubs.rsc.org/en/Content/ArticleLanding/2015/CP/C5CP00932D#!divAbstract.